uOttawa

L'Université canadienne
Canada's university

FACULTÉ DES ÉTUDES SUPÉRIEURES ET POSTOCTORALES

uOttawa

L'Université canadienne
Canada's university

FACULTY OF GRADUATE AND POSDOCTORAL STUDIES

Zhaoqing Jin

AUTEUR DE LA THÈSE / AUTHOR OF THESIS

M.Sc. (Biology)

GRADE / DEGREE

Department of Biology

FACULTÉ, ÉCOLE, DÉPARTEMENT / FACULTY, SCHOOL, DEPARTMENT

Hourglass Cell Development in the Soybean Seed Coat

TITRE DE LA THÈSE / TITLE OF THESIS

Dr. Doug Johnson

DIRECTEUR (DIRECTRICE) DE LA THÈSE / THESIS SUPERVISOR

Dr. Shea Miller

CO-DIRECTEUR (CO-DIRECTRICE) DE LA THÈSE / THESIS CO-SUPERVISOR

EXAMINATEURS (EXAMINATRICES) DE LA THÈSE / THESIS EXAMINERS

Dr. M. Paulin-Levasseur

Dr. Michael Jonz

Dr. Brian Miki

Gary W. Slater

Le Doyen de la Faculté des études supérieures et postdoctorales / Dean of the Faculty of Graduate and Postdoctoral Studies

Hourglass Cell Development in the Soybean Seed Coat

Zhaoqing Jin

Thesis submitted to the
School of Graduate Studies and Research
University of Ottawa
In partial fulfillment of the requirements for the
Master of Science in Biology

Ottawa-Carleton Institute of Biology

Thèse soumise à
l'École des études supérieures et de la recherche
Université d'Ottawa
En vue de l'obtention de la maîtrise ès sciences biologie

L'Institut de biologie d'Ottawa-Carleton

February 2008

Your file Votre référence
ISBN: 978-0-494-48608-5
Our file Notre référence
ISBN: 978-0-494-48608-5

ABSTRACT

Hourglass cells (HGCs) are one of three main cell types in the soybean seed coat. We have studied their structure during the early phases of seed coat development, from 9 to 45 days post anthesis (dpa), by four different microscopic techniques. At 9dpa HGCs resemble typical plant cells but from 12-18dpa they under go rapid changes in their internal and external structure. By 18dpa they have assumed the typical hourglass shape with thick cell walls composed of layers of pectic material, intercellular air spaces and large central vacuoles. By 45 dpa, all organelles in HGCs have been degraded. Additional experiments have shown that plasmodesmata connect all cell types and that soybean peroxidase is localized to the HGC.

These results increase our understanding of the structure and development of the HGC and will be valuable for future studies on protein targeting to components of the endomembrane systems within them.

Résume

Les cellules Hourglass (HGCs) font parties des trois principaux types de cellule de recouvrement des graines de soja.

Nous avions étudier leur structure durant les premiers stade du développement de ce tissu, pendant la période post anthère (ppa) de 9 á 45 jours, ayant recourt á quatre différentes techniques microscopiques.

Au début des 9 ppa les HGCs ressemblent a des cellules végétales typiques. Pendant les 12-18 ppa il y a un changement rapide tant que dans leur structure interne qu'externe. A partir du 18 ppa on a la forme typique hourglass avec des parois cellulaire épaisses composées de couches de matériel pectineux, espace intercellulaire et de larges vacuoles centrales. Apres le 45 ppa toutes les organelles des HGCs sont détruites. Des expériences supplémentaires ont montrées que le plasmodesmata relie toute sorte de cellules et que la peroxidase de soja se trouve dans les HGC.

Ces résultats nous aident á comprendre la structure et le développement des HGC et par la de mieux encadrer les futures études ciblant les protéines des composantes du système endo-membranaire entourant.

ACKNOWLEDGEMENTS

I thank, first and foremost, Dr. Douglas Johnson and Dr. Shea Miller for their enduring patience and guidance. Their willingness to allow me to follow my path of interest has been crucial to my development as a scientist and a thinker. It has been a most enjoyable trip due in large part to their influence and willingness to share their knowledge. I thank the members of my committee, Dr. Brian Miki and Dr. Micheline Paulin-Levasseur, for being approachable and interested in discussing my project.

I am very grateful to Ann-fook Yang and Denise Chabot for their time and effort in training me in the techniques of electron microscopy. I would like to thank Jaimie, Loreta, Manisha and Shuyou for all their support, discussions and cooperation.

I especially thank my best friend and wife, Yanfen, for giving me much help, support and love. I also want to express my cordial thanks to my parents who are in China for their infinite care and love.

TABLE OF CONTENTS

LIST OF TABLES

LIST OF FIGURES

LIST OF ABBREVIATIONS

Abbreviations	Full Name
CCD	Charge-coupled device
CTPP	C-terminal propeptide
DNA	Deoxyribonucleic acid (delete, standard)
dpa	Days post anthesis
epep	Soybean cultivar homozygous (recessive) for no soybean peroxidase activity
EpEp	Soybean cultivar homozygous (dominant) for high soybean peroxidase activity
ER	Endoplasmic reticulum
ESEM	Environmental scanning electron microscope
FAA	Formalin-Aceto-Alcohol
GFP	Green fluorescent protein
GMO	Genetically modified crops
HGC	Hour glass cell
ISAAA	International Service for the Acquisition of Agri-biotech Applications
LM	Light microscopy
LV	Lytic Vacuole
mh	million hectares
NTPP	N-terminal propeptide
PBS	Phosphate buffered saline solution
PBSO	0.1M PBS+ 0.1% ovalbumin

PCD	Programmed cell death
PSV	Protein storage vacuole
SBP	Soybean peroxidase encoded by the *Ep* gene
SEM	Scanning electron microscopy
TBA	Tertiary butyl alcohol
TEM	Transmission electron microscopy
TIP	Tonoplast intrinsic protein

GENERAL INTRODUCTION:

Soybean *(Glycine max* L. Merrill*)* is one of the world's premier agriculture crops. It is widely grown for the oil and protein derived from its seeds and is the major source of protein feed supplement for livestock (Shao et al., 2007). Soybean is the 4th most important crop, just behind wheat, canola, and corn, in Canada. Canadian soybean production in the 2006- 2007 crop year was a record high of 3,466,000 tonnes, and the average price was $262/ ton (http://www.canadiansoybeans.com/production.php) contributing over $900 million to the Canadian economy. From 2001 to 2006, Canadian soybean exports increased from ~0.5 to ~1.3 million tonnes (http://www.soybean.on.ca/marketing_info.php). According to ISAAA (International Service for the Acquisition of Agri-biotech Applications) GMO (genetically modified organism) herbicide-tolerant soybean, mainly glypohosate and glufosinate resistance, continues to be the principal GMO crop world-wide in 2006 occupying 58.6 million hectares(mh) (57% of area devoted to GMO crops) followed by maize (25.2 mh), cotton (13.4 mh) and canola (4.8 mh) (James, 2006).

About 60% of soybean by dry weight is oil (20%) and protein (40%). The oil is used mainly as edible oil while the protein is used mainly as an animal feed supplement and in human foodstuffs (soy protein is considered to be complete protein with all the essential amino acids, http://en.wikipedia.org/wiki/Soy_beans#_note-17). During processing hulls are usually removed as a waste. In some soybean cultivars such as Harosoy63, 5% of the total soluble protein in the seed coat is soybean peroxidase (SBP) encoded by the *Ep* locus which has commercial value as a catalyst for the oxidative polymerization of cardanol that is used for anti-biofilm coating material (Kim et al., 2003) although other potential markets may exist such as the treatment of industrial wastewaters containing phenolic contaminants

(Wright and Nicell, 1999). The market for this enzyme is limited so that seed coats add little value for farmers or processors. In fact the major use for seed coats is as a dietary ingredient for animals.

The seed coat consists of only a few cell types and recent research on soybean seed coats indicates that hourglass cell (HGC) is the site of expression and storage of SBP (Gijzen et al., 1993). These results suggest that the accumulation of heterologous proteins in the seed coat can be achieved by using signals derived from SBP for controlling their expression and targeting. Therefore, by using molecular biotechnology, soybean seed coats could become a potential reservoir for proteins for the production and storage of other high-valued proteins or novel biochemicals, and could be introduced into a market that already accepts transgenic soy.

Success in this program could have a tremendous economic impact. However, in spite of a number of studies on soybean seed coat development, information about HGC development remains incomplete. A crucial part of this project is a better understanding of the hourglass cell of the seed coat, as protein accumulation is thought to occur in vacuoles in this cell. We need to know "how does the cell develop?" and "what is its capacity for storing protein?" The purpose of this thesis is to study the ultrastructure of the hourglass cells, and the secretory process of the hourglass cells in soybean seed coats. A developmental study of the changes in the structure of the hourglass cells during the period of seed filling will provide valuable information about this crucial cell type, and help to answer the questions asked above.

CHAPTER ONE: LITERATURE REVIEW

Seed development is a genetically programmed process correlating with changes in metabolite level. Although the structure and composition of seed coats varies among different plant species, seed coat development undergoes similar phases in relation to the embryo and endosperm. For example, the legume seed always develops following three phases: 1. the seed coat and endosperm develop; 2. the development of the embryo, maturation of the seed coat; 3. the maturation of the embryo (Moise et al., 2005; Weber et al., 2005). More details of soybean seed coat development, especially the hourglass cell development in soybean seed coat will be introduced in this thesis.

1.1 Soybean Seed Coat Morphology and Development

As an important part in a plant seed, the seed coat plays a fundamental role in the life cycle of plants by controlling the development of the embryo and determining seed dormancy and germination (Egley et al., 1984; Stabell et al., 1996; Moise et al., 2005). Usually, the embryos in seeds are wrapped closely by their hard seed coats which are impervious to water and gases, so seeds will not germinate until their seed coats are altered physically by outside environments. The seeds of soybean have been the subject of extensive research for many years (Raper and Patterson, 1986; Jurgonski et al., 1997; Reinprecht et al., 2006; He et al., 2007; Malencic et al., 2007), and some research on biochemical and morphological studies in soybean seed coats have been reported in recent years (Gizjen et al., 1993; Miller et al., 1999; Moise et al., 2005, Shao et al., 2007; Liu et al., 2007), but the details of the hourglass cell development in soybean seed coats are few in number.

1.1.1 Mature Soybean Seed Coat Morphology

The mature soybean seed is typical of many legumes. Usually, the seeds are oval in shape and their seed coats are buff to yellow in colour although darker seeds are known. Developing seeds are attached by the funiculus to the two large vascular bundles in the pod placenta. The mature seed coat has a clear scar called the hilum, formed as a result of the seed separating from the funiculus (Fig. 1.1A).

Soybean seed coats originate from integuments that surround the ovary prior to fertilization (Moise et al., 2005). These integuments then develop into different cell layers of maternal origin. Following fertilization, each layer has specialized cell types and functions. The seed coat of the mature soybean has five distinct cell layers: an epidermal layer of palisade cells, or macrosclereids, a sub-epidermal layer of hourglass cells, or osteosclereids, a few layers of parenchyma, an aleurone layer and a layer consisting of crushed cell remnants of endosperm (Fig. 1.1B) (Williams, 1950; Corner, 1951). This pattern is conserved in many legumes such as lupin, pea, milkvetch, common bean, white popinac (Moise et al., 2005) and *Senna corymbosa* (Rodriguez-Pontes, 2007).

The palisade layer, the outermost layer of the legume seed, is found under the waxy cuticle. It is composed of thick-walled palisade cells which contribute to the mechanical strength of the seed coat, although these cells are dead at this stage (Algan and Buyukkartal, 2000; Shao et al., 2007). A second palisade layer, the "counter palisade", is present at the hilum.

Adjacent to the palisade layer are the thick-walled hourglass cells. Like palisade cells, hourglass cells are all dead and also play a role in the mechanical strength of the seed coat (Shao et al., 2007). There are no hourglass cells at the hilum.

The parenchyma layer, which is thinnest at the end of the seed coat opposite the hilum, consists of 6–8 layers of thin-walled, tangentially elongated parenchyma cells. The function of the parenchyma layer is not clear (Moise et al., 2005).

1.1.2 Soybean Seed Coat Development

The morphological studies carried out by Miller et al. (1999) used light microscopy of stained material to describe changes that occur in the soybean seed coat during the first 3 weeks after fertilization when most of the dramatic changes occur. During this time, the outer integument, initially containing three similar tissue layers, differentiates into the palisade layer, the thick-walled hourglass cells and the parenchyma layer. As my studies are based upon this previous work, a brief description of the published work of Miller et al. (1999) is provided.

Figure 1.1 Schematic diagrams of the soybean seed and seed coat

This figure illustrates the anatomy of soybean seed attachment and the cross section of the mature seed. (A) Sketch of a typical transverse section of an entire soybean seed. CT, cotyledon; F, funiculus; H,hilum; TB, tracheid bar; VB, vascular bundles (Thorne, 1981). (B) This figure illustrates the morphological details of a mature soybean seed coat. al, aleurone cells; cut, cuticle; hyp, hourglass cells of hypodermis; int sp, intercellular space; lu, lumen; pal, palisade; par, compressed parenchyma cells; par end; remains of parenchyma cells of endosperm (Souza and Marcos-Filho, 2001).

A

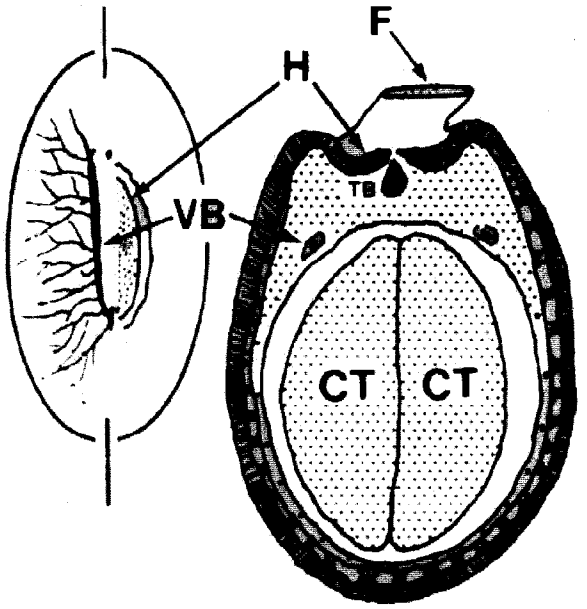
F
H
VB
TB
CT
CT

B

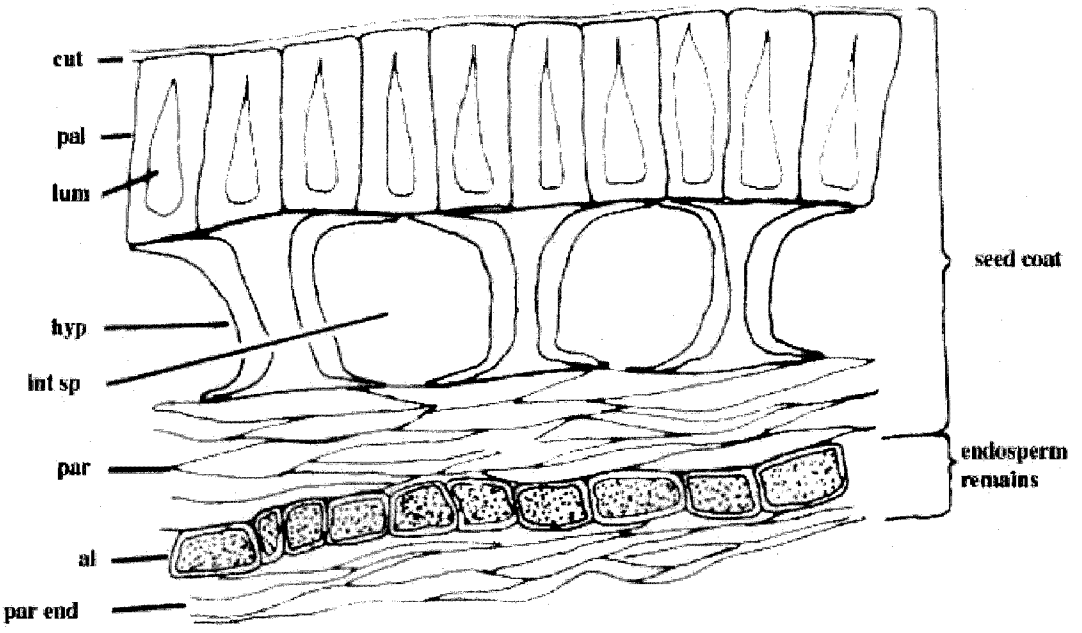
cut
pal
lum
hyp
int sp
par
al
par end
seed coat
endosperm
remains

hypodermis appear in the cells opposite the hilum, at the bottom of the seed (Fig. 1.2C). At 12 dpa, the palisade cells have distinct thin-and thick cell walls and clear vascular region. Although hourglass cells begin to differentiate from the hypodermis near the top, or hilum portion, of the seed, they do not show any typical characters of mature hourglass cells (Fig. 1.2D). At 15 dpa, the seed coat shows three typical layers. The cell wall of palisade and hourglass cells becomes thicker; obvious air spaces are visible between the hourglass cells when the hourglass cells finish most of their differentiation; the thin- and thick-walled parenchyma and vascular region are clearly distinguishable (Miller et al., 1999); large air spaces are also starting to appear between the thin-walled parenchyma cells (Fig. 1.2E). After 18 dpa, the differentiation rate and further changes of the structure of the soybean seed coat are more inconspicuous. At 30 dpa, the parenchyma is beginning to be crushed. At 45 dpa, the seed coat is completely mature. The most prominent features are the hourglass cells and palisade layer, and only a few layers of slightly flattened thin-walled parenchyma remain.

While these studies led to a more detailed description of early development of HGCs in soybean seed coat, they were limited by the use of light microscopy and could not describe the details of the ultrastructure changes of HGCs. Thus in order to understand the ultrastructural changes that accompany HGC development more clearly we need to turn to techniques such as Transmission electron microscopy (TEM) and Scanning electron microscopy (SEM). Comparisons between light microscopy and electron microscopy will be discussed in Section 1.5.

Figure 1.2 Light micrograph of a cross section through a soybean seed coat

This figure illustrates the morphological details of a soybean seed coat at anthesis, 6, 9 ,12and 15 days post anthesis. (A) Cross section of seed coat at anthesis, stained with PAS and Light Green. Bar = 20μm. (B) Cross section of whole soybean seed coat at 6 dpa, stained with Toluidine Blue. Bar = 100μm (C) Cross section of seed coat at 9 dpa, stained with Toluidine Blue. Bar = 100μm (D) Cross section of seed coat at 12 dpa, stained with PAS and Light Green. Bar = 50μm (E) Cross section of whole soybean seed coat at 15 dpa, stained with PAS and Light Green. Bar = 100μm. p, palisade layer; h, hourglass cells; pa, parenchyma; vb, vascular bundle; k, thick-walled parenchyma; en, endothelium; ii, inner integument; em, endosperm; ep, epidermis; hp, hypodermis; s, starch granules sc, sclerenchyma; oi, outer integument; ie, inner epidermis. These figures were taken from Miller et al., 1999.

A

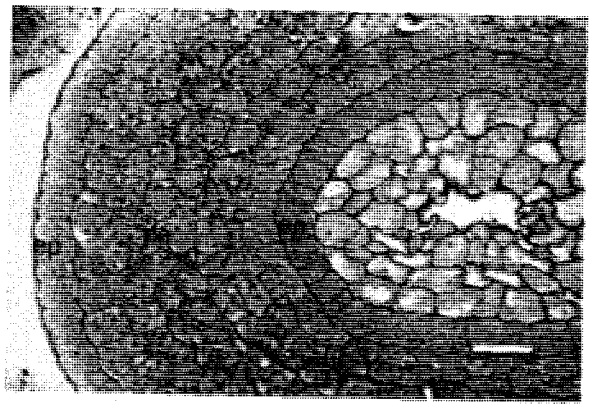

B

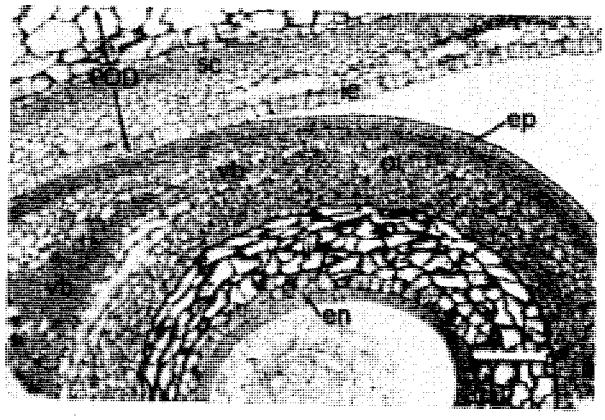

C

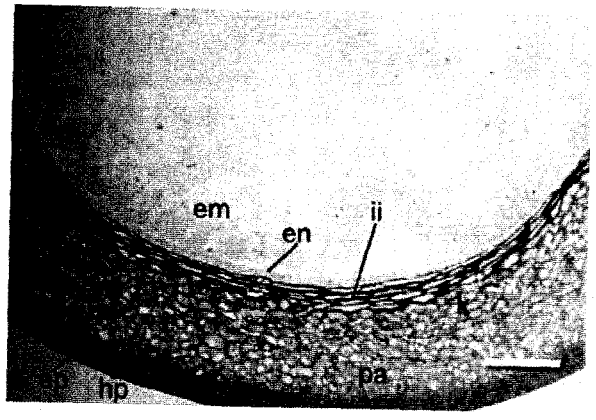

D

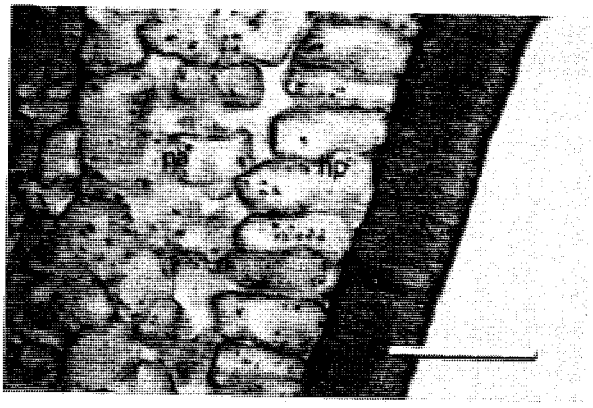

E

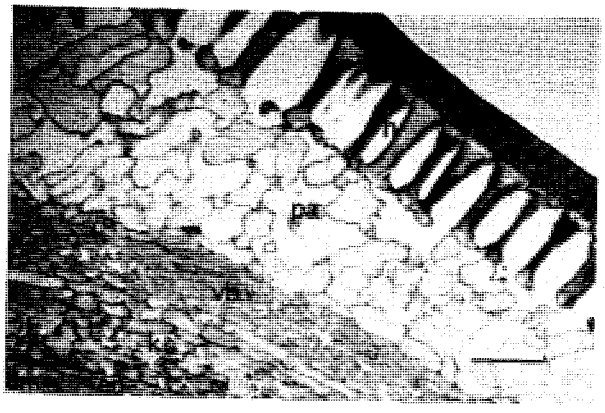

1.1.3 Hourglass Cells in Soybean Seed Coat

The hourglass cells in soybean seed coat arise from the outer-cell layer of the inner integument and differentiate from the hypodermis near the top of the seed at 12 dpa. They are also named pillar cells, or osteosclereids, or lagenosclereids, depending on the thickness of the cell-wall and precise shape (Moise et al., 2005). The term "hourglass cell" will be used throughout this thesis. Between 12 and 15 dpa, the hourglass cells finish their transformation and at 18 dpa, hourglass cells are well defined (Miller et al., 1999; Zeng et al., 2004). In mature soybean seed coats, HGCs are separated with wide intercellular air spaces and are larger than palisade and parenchyma cells, but they are absent under the hilum cleft (Souza and Marcos-Filho, 2001; Shao et al., 2007). van Dongen et al. (2003) employed cryogenic specimen preparation techniques for SEM which allow observation of the sample in its "natural" hydrated state. They observed both liquid-filled and air-filled intercellular spaces among parenchyma cells during pea seed coat development but did not state whether the same liquid-filled and air-filled intercellular spaces were observed between HGCs. Only air-filled spaces between HGCs could be found from their cryo-SEM pictures (Figure 3, van Dongen et al. 2003), but this evidence is not strong enough to confirm whether the volume between HGCs is aqueous or air-filled in developing seed coats at all stages. A more thorough study using cryo-SEM focused on HGCs could be an effective way to determine whether the intercellular spaces between developing HGCs are liquid-filled or air-filled or a mixture of both types and what is their developmental fate. The hourglass cell has a dense cytoplasm and a large central vacuole. It may function to synthesize nutrients for the developing embryo, as suggested by the presence of numerous starch grains in the hourglass cells during embryogenesis (Algan and Buyukkartal, 2000; Wang and Grusak, 2005).

However, the main function of hourglass cells in the mature seed may be to provide mechanical strength to the seed coat (Moise et al., 2005).

HGCs contain proteins (Miller et al., 1999) such as seed coat peroxidase that are released during seed imbibition (Gijzen et al., 1997). A single isozyme of seed coat peroxidase accumulates in large amounts (5% of the total soluble protein) in the hourglass cell as glycoproteins (Gijzen et al., 1993), and the peroxidase can be stored stably for a long period in the dried seed coat. It has been found that the hull of wild-type (*EpEp*) soybean cultivars has very high peroxidase activity, 100-fold greater than that of mutant (*epep*) soybean cultivars containing low activity. Although SBP is less expressed in *epep* cultivars, there are, nevertheless, other peroxidases, which are the likely source of the low level activity preserved in them. Hulls from wild-type (*EpEp*) cultivars with high activity could be used as a commercial source of peroxidase for industrial products.

Hourglass cells have been described in the seed coats from a large number of legumes such as lupin (Clements et al., 2004), pea (van Dongen et al., 2003), milkvetch (Miklas et al., 1987), common bean (Yeung, 1990), white popinac (Serrato-Valenti et al., 1995), yam bean (Ene-Obong and Okoye, 1993), pulse (Gupta et al., 1985), *Senna corymbosa* (Rodriguez-Pontes, 2007) and many others (Paria et al., 1997; Sornsathapornkul and Owens, 1999). While direct comparisons of HGCs in these species are made difficult due to differences in sample preparation and stage of seed coat development, it appears that the HGC structure is widely maintained throughout the legumes.

1.2 Plant Cell Structure

Cells are the structural and functional units of all living organisms. Because of their small size, most cells can only be observed with the aid of a microscope. Plant cells are quite different from the cells of the other eukaryotic organisms.

In general, a typical plant cell includes these distinctive features: a large central vacuole (enclosed by a membrane, the tonoplast), which maintains the cell's turgor and controls movement of molecules between the cytosol and sap; a cell wall composed of cellulose and other polysaccharides, protein, and in many cases lignin, deposited by the protoplast on the outside of the cell membrane; the plasmodesmata, linking pores in the cell wall that allow each plant cell to communicate with other adjacent cells; and plastids, especially chloroplasts that contain chlorophyll, the pigment that gives plants their green color and allows them to perform photosynthesis.

1.2.1 Plant Cell Walls

The presence of a cell wall is one of the most important distinguishing features of plant cells. The plant cell wall serves a variety of functions, such as giving cells rigidity and strength and protecting the intracellular contents. The cell wall provides a porous medium for the circulation and distribution of water, minerals, and other nutrients, limits the entry of molecules that may be toxic to the cell and protects the plant from diseases (Cosgrove, 2001; Keegstra et al., 1973).

Many plant cells form two types of cell walls that differ in function and in composition. The primary walls surround growing and dividing plant cells. These walls provide mechanical strength. The main chemical components of the primary plant cell wall

include cellulose, pectins and cross-linking glycans. The secondary walls are often deposited inside the primary cell wall as a cell matures. They are further strengthened by the incorporation of lignin. The primary cell wall is thinner and more pliant than the secondary cell wall, and is sometimes retained in an unchanged or slightly modified state without the addition of the secondary wall, even after the growth process has ended. The cytoplasms of adjacent cells are usually connected by plasmodesmata that run through the layers of the cell walls (Carpita and Gibeaut, 1993; Cosgrove, 2001). Plasmodesmata are especially common in the walls of columns of plant cells and provide routes for communication and nutrient transfer between plant cells. The fine structure of plasmodesma consists of a cylindrical membrane which is continuous with the plasma membrane of the adjacent cells, and within this membrane channel is a sieve narrower element called the desmotubule (Tilney et al., 1991; Kim et al, 2002; Heinlein, 2002). The thick cell wall is one of the most important characters of HGCs, but how their cell walls change during development is still unknown.

1.2.2 The Endomembrane System in Plant Cells

The endomembrane system is a collection of membranous structures involved in transport within the cell and to the outside. The major components of the endomembrane system of higher plant cells are generally considered to include the endoplasmic reticulum (ER), the Golgi apparatus, and their transition elements, with the various vesicles, vacuoles, and other organelles derived from them. The nuclear envelope is also included in most discussions as is the plasmalemma , although this is not strictly an endomembrane. The membranes of the semiautonomous organelles, the mitochondria and plastids, are usually excluded from general consideration of the endomembrane system (Harris, 1984). The

endomembrane system plays a very important role in moving materials around the cell, notably proteins and membranes.

Within plants, the ER is surrounded by large vesicles that are free or attached to the plasma membrane (Yaklich et al., 1998) and play a central role in distributing protein to several compartments via the endomembrane or secretion pathway. Soluble proteins that are targeted to the plant secretory system have an N-terminal propeptide (NTPP) which directs co-translational import into the ER (Vitale and Hinz, 2005). In addition, Claude et al. (2005) found that C-terminal propeptides (CTPP) functioned in the transport and vacuolar targeting of recombinant proConA in jack bean cotyledons. Brandizzi et al. (2004) described vacuolar soluble protein sorting mediated by the plant cell endomembrane system (Fig. 1.3). Protein is transported to pH-neutral (Surpin and Raikhel, 2004) Protein Storage Vacuoles (PSVs) via the ER (Route 1) or ER and Golgi (Route 2). Transport to the Lytic Vacuole (LV) via the ER and Golgi (Route 4) is mediated by the prevacuolar compartment (PVC) (Matsuoka et al., 1995). Protein is also transported to plasma membrane via ER and Golgi either mediated by PVCs (Route 4, 5) or not (Route 3). Following translocation the signal peptide is removed. The NTPP is cleaved in the ER while the CTPP is removed in the vacuole.

Clearly, the endomembrane system plays a very important role for protein storage and transport during plant cell development. Although the morphology of the endomembrane system in many higher plant cells has been studied before, the details of the endomembrane system in HGCs and its role in trafficking are still unknown.

1.2.3 Protein Storage Vacuoles and Lytic Vacuoles

Vacuoles, as one of the major features of the plant cell, are multifunctional organelles. In vegetative cells, vacuoles occupy much of the cell volume and maintain the cell turgor.

During cell development, vacuoles sequester and inactivate toxic compounds, participate in programmed cell death, accumulate defence proteins and thousands of secondary metabolites, and store proteins to be used later as a source of reduced nitrogen (Marty, 1999; Hatsugai et al., 2004; Bethke and Jones, 2000).

In fact, all these seemingly contrasting functions can be performed by the same organelle, which can explain why plant cells have different types of vacuoles, and these vacuoles can coexist in a single cell. Vacuoles can generally be divided into two main categories: (i) Lytic Vacuoles (LVs) are acidic compartments, rich in hydrolases and can be regarded as the equivalent of mammalian lysosomes; and (ii) Protein Storage Vacuoles (PSVs), are found in storage organs and can store large amounts of protein (Vitale and Hinz, 2005; Jolliffe et al., 2005). Vacuoles can be characterized by the presence of specific tonoplast intrinsic proteins (TIPs): α-TIP is associated with PSVs, whereas γ-TIP is found in LVs (Paris et al., 1996). The TIPs function as aquaporins (Chrispeels and Maurel, 1994).

The biological roles of the LVs present in most cells and PSVs in seed cells are rather clear (Herman and Larkins, 1999; Marty, 1999). LVs are important for maintenance of turgor pressure, storage of metabolites, sequestration of xenobiotic compounds, and digestion of cytoplasmic constituents (Park et al., 2004). PSVs are specialized vacuoles devoted to the accumulation of large amounts of protein in the storage tissues. PSVs are typical of seeds that store proteins in cotyledons or living endosperm but they can also be abundant in other tissues, such as bark, tubers, leafs or pods, when there is a need to accumulate storage compounds transiently. Seed PSVs are easily recognizable in electron micrographs because their content is electron opaque due to the high concentration of protein. PSVs often also contain large amounts of toxic proteins (such as lectins, protease inhibitors and ribosome inactivating proteins) which probably evolved to protect seeds from predators. PSVs seem to

have a higher pH than do LVs and, during protein accumulation, lower hydrolytic activity (Vitale and Hinz, 2005).

There are some interesting relationships between LVs and PSVs during plant cell development. In general, PSVs change their identity and seem to be transformed into LVs during the mobilization of storage proteins. On the other hand, Hoh et al. (1995) found LVs were present in immature pea *(Pisum sativum)* cotyledon cells, but during maturation they were replaced by PSVs. In a soybean cotyledon cell, a single large vacuole was present and occupied a considerable portion of the space at an early stage. During seed growth, the large vacuole was replaced by small PSVs where storage proteins accumulate (Mori et al., 2004).

Despite a number of studies examining different vacuoles in soybean seeds (Mori et al., 2004; Maruyama et al., 2006; He et al., 2007), information on PSVs and LVs in soybean seed coat development is incomplete, and the localization of SBP in HGCs remains in question.

Figure 1.3 Schematic diagram of the endomembrane system in plant cells

This figure illustrates the endomembrane organelles of the plant secretory pathway in plant cells. CW, cell wall; ER, endoplasmic reticulum; G, Golgi apparatus; PM, plasma membrane; N, nucleus; PVC, prevacuolar compartment (Brandizzi et al., 2004).

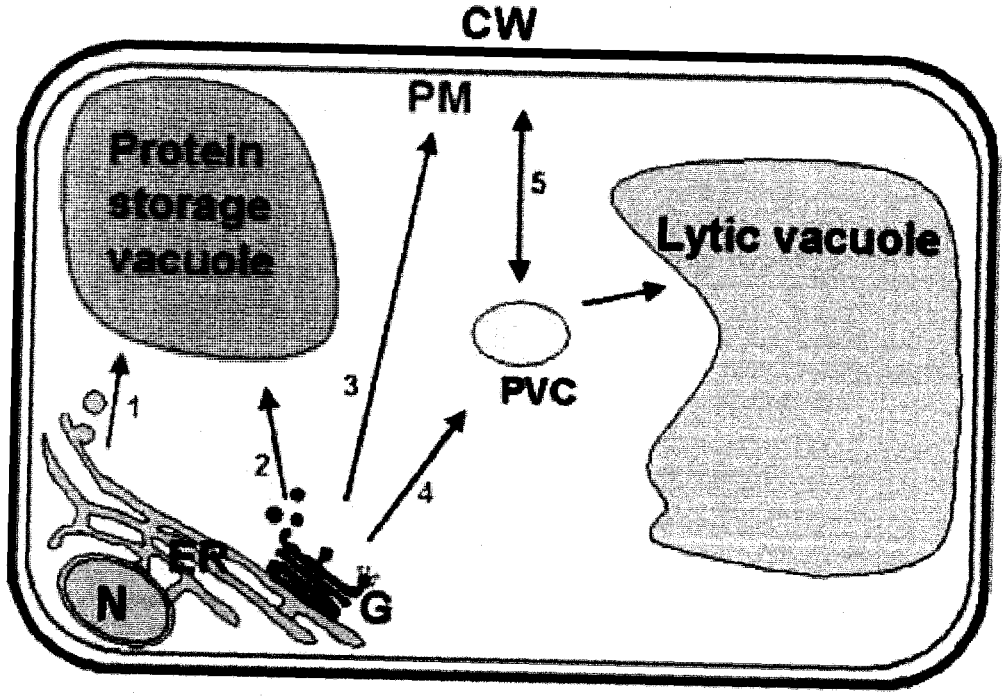
CW
PM
Protein storage vacuole
5
Lytic vacuole
PVC
1
2
3
4
ER
N
G

1.3 Soybean Seed Coat Peroxidase

Peroxidases, a class of enzymes found in animals, plants and micro-organisms, catalyze oxido-reduction between H_2O_2, which is naturally produced as a byproduct of oxygen metabolism in living plant cells for reasons related to plant disease resistance (hypersensitive response) and senescence (Levine et al., 1994; Alesandrini et al., 2002), and various reductants (Hiraga et al., 2001). Plant peroxidases are a family of isozymes found in all plants, occurring as heme-containing monomeric glycoproteins. Several physiological functions for peroxidases in plants have been reported, such as removal of H_20_2, oxidation of toxic reductants, biosynthesis and degradation of lignin in cell walls (Mader and Ambergfisher, 1982; Lagrimini, 1991), defence against pathogen or insect attack (Dowd, 1997) and extensin polymerization (Fry, 1986).

Soybean seed coat peroxidase (SBP) is a 37 kD glycoprotein expressed in the seed coat of soybean at 20 dpa (Gillikin and Graham 1991; Gijzen et al., 1993). SBP has high thermal and pH-stability (pH: 2-11), can function in organic solvents, and shows a number of unique catalytic properties (Welinder and Larsen, 2004). SBP belongs to the family of class III plant peroxidases that can oxidize a wide variety of organic and inorganic substrates using hydrogen peroxide. Although the precise function of SBP in seed coats is not known, possible roles in several processes such as lignification, suberization and cell defense responses have been postulated (Gijzen et al., 1993; Henriksen et al., 2001; Welinder and Larsen, 2004). However, Gijzen et al. (1993) found that *EpEp* soybean cultivars did not have obvious differences in seed coat structure, rigidity, permeability, or lignification compared with *epep* cultivars. In addition they did not find any evidence to associate differences in the gross or microscopic structure of the seed coat with the *Ep* locus. Thus the exact role(s) of

SBP remains unproven as does the mechanism(s) by which hydrogen peroxide is supplied for the postulated role.

SBP activity is controlled by the *Ep* locus. SBP is present at high concentrations in the soybean seed coat depending on cultivar. Histochemical localization of SBP activity revealed that the enzyme accumulates predominantly in the hourglass cells of the subepidermis in *EpEp* soybean cultivars (Gijzen et al., 1993). SBP shows more than 70% amino acid sequence identity to peroxidases from other legumes (Welinder and Larsen, 2004). For instance, the soybean sequence is very closely related to four peroxidase cDNAs isolated from alfalfa, with 65–67% homology at the amino acid level (Gijzen, 1997).

Although the location of SBP within the cell has not been determined experimentally two lines of evidence suggest transport via the ER to Golgi to the vacuole. First, analysis of the primary protein sequence (Gijzen et al., 1993, 1997) suggests the presence of an NTPP and CTPP. Welinder and Larsen (2004) have shown that in mature SBP these sequences are lost as would occur during transport via the ER to the vacuole (Gray et al., 1996; Welinder and Larsen, 2004). Secondly, SBP is a heavily glycosylated protein. Gray et al. (1996) demonstrated the presence of mannose, xylose and fucose suggesting that SBP had passed through the Golgi on its way to the vacuole.

A detailed histochemical examination of cells and tissues of the developing seed coat revealed the spatial and developmental pattern of *Ep* peroxidase expression in the hourglass cell (Gijzen et al., 1993, 1997). The difference in activity is conditioned by a single gene pair, designated *Ep/ep* (Gizjen et al., 1993). The mutations in the peroxidase-deficient lines were found to result from deletions in the promoter region of *Ep* peroxidase genes rather than defects downstream of transcription (Gijzen et al., 1997).The deficient lines produced normal-looking hourglass cells and did not under-perform compared with wild-type (*EpEp*)

soybean varieties (Gijzen et al., 1993, 1997). So *epep* mutant lines could make excellent hosts for the production of large amounts of protein using *Ep* peroxidase regulatory elements for expression in hourglass cells.

In 1999, a second peroxidase gene was isolated (*Prx2*) that is also highly expressed in developing seed coat tissues (Gijzen et al., 1999). Sequence analysis of *Prx2* cDNA indicates that this transcript encodes a cationic peroxidase. By comparing the abundance and localization of the *Ep* and *Prx2* transcripts, it was shown that the expression of *Ep* begins in a small number of cells flanking the vascular bundle in the seed coat, spreads to encircle the seed, and then migrates to the hourglass cells as they develop. Expression of *Prx2* occurs throughout development in all cell layers of the seed coat, and is also evident in the pericarp and embryo. The *Prx2* enzyme is either insoluble in a catalytically inactive form, or is subjected to degradation during seed maturation (Gijzen et al., 1999; Moise et al., 2005).

SBP could provide an alternative to horseradish peroxidase in many industrial applications because of its high stability and activity, and it is present at high concentration in the soybean seed coat in some cultivars (Gijzen, 1997; Gijzen et al., 1993). Due to its high thermo- and pH-stability it can be easily purified from soybean hulls (Henriksen et al., 2001; Nissum et al., 2001; Welinder and Larsen, 2004).

1.4 Seed Coat Development Studied using Microscopy

The light microscope is probably the most well-known and well-used research tool in biology. With the different staining dyes, the light microscope not only can provide spectacular views, but information about the chemical composition of cells. As a common tool in cell biology, light microscopy (LM) has many advantages, such as relatively low price, convenient operation, and fast results, but its low magnification limits its application

as it is difficult to resolve detail in many organelles, such as ER, Golgi and plasmodesma within cells. Miller et al. (1999) studied the early development of soybean seed coats using light microscopy.

EM has been used as an experimental tool to study seed coat structure in legumes. Thorne (1981) observed the structure of the mature soybean seed coat using TEM and SEM and described details of the three cell layers in soybean seed coat. Algan and Buyukkartal (2000) studied seed coat development in the natural tetraploid *Trifolium pratense* L. using TEM and showed that HGCs had thin cell walls and were highly vacuolate with densely staining cytoplasm at early stage, but that the cytoplasm disappeared in all cells at the mature seed stage. van Dongen et al. (2003) used light microscopy and SEM to monitor the apoplastic transport of nutrients between seed coats and cotyledons during seed coat development in pea. While these results have been very important for our understanding of the seed coat structure, no systematic study has used TEM and SEM to investigate the changes in seed coat structure during development.

SEM is a type of electron microscope capable of producing high-resolution images of a sample surface. SEM images have a characteristic three-dimensional appearance and are useful for judging the surface structure of the sample (http://en.wikipedia.org). Although SEM can zoom in over 7,000 times (7,000 X) and take high quality pictures, it just scans the surface of samples and shows only black and white photos.

TEM is an imaging technique whereby a beam of electrons is transmitted through an ultra-thin section (~10 nm) of the specimen, then an image is formed, magnified and directed to appear either on a fluorescent screen or layer of photographic film, or to be detected by a sensor such as a CCD camera (http://en.wikipedia.org). TEM is the most effective way to study the endomembrane system of higher plant cells because of its high magnification (over

1,000,000 X). In this work, we used Vacuum Microwave Processing for TEM. Microwave technology reduces the time required for sample processing by over 90%, when compared to routine processing protocols (Ted Pella, Inc., Redding, CA, USA). However, the TEM process is still much more complex and the preparation time is longer than that of other microscopy techniques.

Confocal microscopy is an imaging technique used to increase contrast and/or to reconstruct three-dimensional images by using a spatial pinhole to eliminate out-of-focus light or flare in specimens that are thicker than the focal plane (http://en.wikipedia.org). Confocal microscopy can show colorful images of the whole living cells, so it is the first choice for observing fluorescent staining in plant cells. But, sometimes the autofluorescence of cell organelles interferes with the components of interest.

As outlined above all four techniques have their advantages and disadvantages. But when used together to gather complementary information, they are still the most effective way to study cell biology and provide complete information about cell structures and contents. For example, we can use LM combined with the use of stains to examine cell contents and morphology, as well as analyze larger scale specimens unsuitable for SEM and TEM imaging; use SEM to scan cell surfaces; use TEM to detect cell ultrastructure and its endomembrane system; and then use confocal microscopy to observe dynamic processes in living cells.

1.5 Thesis Objectives

The objectives of this research are as follows:

1) Investigate the development and composition of the hourglass cell

Different dyes were used to stain HGCs. LM and confocal microscopy were used to judge the composition in HGCs during the development. This is an extension of the work of Miller et al. (1999).

2) Investigate the developing HGC by scanning electron microscopy and transmission electron microscopy

Changes in HGC surfaces were documented by SEM during soybean seed coat development. TEM was used to observe the changes of the ultrastructure in HGCs during soybean seed coat development.

3) Confirm the localization of SBP within the HGC

TEM, confocal microscopy and immunogold labeling were used to compare and localize SBP in HGCs in wild type (*EpEp*) soybean seed coats.

CHAPTER TWO: MATERIALS AND METHODS

2.1 Plant Material and Propagation

Cultivars (cv) of soybean *Glycine max* (L.) Merrill included in this study were Maple Presto, Harosoy 63 and Jack. Maple Presto was obtained from Dr. E. Cober, Agriculture and Agri-Food Canada, Ottawa, ON, Canada. Harosoy 63 and Jack were obtained from Dr. V Poysa, Southern Crop Protection and Food Research Centre, Agriculture and Agri-Food Canada, London, ON, Canada. Seeds were germinated in moist vermiculite at room temperature and then planted in soil in 127 mm inch pots. Seedlings were grown under fluorescent and incandescent light (300 $\mu E/m^2/s$) for a 12 hour photoperiod in Conviron E15 growth cabinets set at 25°C and 20 °C during the light and the dark cycles respectively. Relative humidity was maintained at 80%. After approximately one week seedlings were transplanted into soil in 127 mm peat pots. The relative humidity of the cabinets was changed to 70% at approximately 35 days post anthesis (dpa) and watering was terminated to allow for seed drying (Miller et al., 1999).

In order to follow seed development, flowers were tagged at each plant node on the day of full anthesis according to the flower staging system described in Table 2.1 (Peterson et al., 1992). Because all flowers at one raceme are not open at the same day, only the first flower was labeled. The largest pod at the labeled raceme was harvested.

All plants were grown, processed and examined using plant growth and microscopy facilities at Agriculture and Agri-Food Canada, Eastern Cereal and Oilseed Research Centre, Ottawa, ON, Canada.

Table 2.1 Stages of soybean flowering

The following table outlines the morphological appearance of soybean flowers at early stages of seed development (Peterson et al. 1992).

Seed Stage (dpa)	Flower
-2	No visible corolla; corolla visible, but not fully extended beyond calyx lobes.
0	Banner petal fully extended; partial opening of banner petal; appears 'hooded'; banner petal completely reflexed.
1	Banner petal collapsed; appears 'hooded'.
2	Margins of banner petal slightly wilted and rolled inward. Small brownish spots visible on banner and / or keel petals.
2-3	More spots, discoloration and wilting along petal edges; parts of petals withered.
3-4	Completely withered petals, no turgid petal tissues visible to eye or with x 10 hand-lens.
4-6	Withered corolla may be torn away or abscised from receptacle by expanding pod.

2.2 Light Microscopy

Soybean seeds for light microscopy were collected at 9, 12, 13, 14, 15, 18, 19, 30 and 45 dpa. The seeds were separated into seed coat and embryo tissues. The seed tissues were cut into 2mm segments as outlined in Table 2.2 and immediately placed into vials of FAA fixative (3.7% (v/v) formaldehyde, 50% (v/v) ethanol, and 5% (v/v) acetic acid). Any seed sections remaining attached to the pod were fixed as a unit.

2.2.1 Fixation and Embedding

Following fixation for 24 hours at room temperature in FAA, seed segments were dehydrated in an ethanol series (Table 2.3A), infiltrated with paraffin/ tertiary butyl alcohol (*tert*-Butanol (99+% A.C.S. Reagent, Sigma) (Table 2.3B), and then infiltrated with Paraplast X-TRA paraffin (Oxford® , MO, U.S.A.) over 2 days (Ruzin, 1999).

Sections (approximate 6-8 μm) of the paraffin embedded samples were cut with a stainless steel knife on a Spencer 820 microtome (American Optical Company, NY, U.S.A.), and mounted on drops of distilled water on Fisherbrand® microscope slides (Fisher Scientific, U.S.A.).

Table 2.2 Preparation of Seed Sections

Processing of soybean seed tissues for fixation in FAA fixative.

Seed Stage (dpa)	Seed Section
9	If the seed is still attached to the pod then pod is cut on either side of the seed. The seed is cut in half, transversally.
12-15	The ends of the seed are cut off and discarded. The remaining seed is cut in half, transversally.
18-30	The ends of the seed are cut off and discarded. The remaining seed is cut into 1-2 mm sections.
45	The ends of the seed are cut off and discarded. The remaining seed is cut into 1-2 mm sections.

Table 2.3A Ethanol dehydration series after FAA fixation (Ruzin, 1999).

Ethanol dilutions were made using anhydrous ethyl alcohol (Commercial Alcohols Inc., Brampton, ON) and distilled water.

% EtOH	Time (h)
50	1-4
70	1-4
90	1-4
95	1-4
100	2-4

Table 2.3B Proceed with Paraffin/ TBA infiltration (Ruzin, 1999).

Infiltration media made with ethanol as in Table 2.3A, *tert*-Butanol (99+% A.C.S. Reagent, Sigma), and paraffin (Paraplast X-TRA, Oxford®, MO)

Step	95% EtOH	100% EtOH	% TBA	% Paraffin	Time (h)
1	50		50		1-4
2		25	75		1-4
3		25	75		1-4
4			100		1-4
5			100		1-4
6			67	33	1-4

2.2.2 Histochemistry

Tissue embedded in paraffin can be stained with dye, however the paraffin is always removed prior to light microscopy. In this work, xylene was used to deparaffinize sections, and then EtOH: xylene mixture and a graded series of decreasing EtOH concentrations were used to hydrate sections. Finally, sections were dried in air and ready for staining.

The stained sections were examined by a Zeiss Axioplan 2 Microscope (Carl Zeiss, Germany). All LM images were taken by a Zeiss Axiocam charge-coupled device (CCD) digital camera mounted on the microscope, and saved in the computer directly.

2.2.2.1 Toluidine Blue O

For observation of general cell structure, sections were stained with Toluidine Blue O (0.05% in 50 mM potassium acetate buffer, pH 4.4) for 2 min, rinsed in distilled water and mounted in glycerol, or air dried and mounted in immersion oil. Toluidine Blue O is a metachromatic, cationic thiazine dye (Green, 1990) that is commonly used for plant structural studies. Cellulose walls appear purple to blue, cytoplasm stains light blue and nuclei stain dark blue.

2.2.2.2 Ruthenium Red

Ruthenium Red (0.05% in distilled water) was used for observing pectin in stained plant cell walls. Slides were stained in the dark until color developed (4-6 min), rinsed in distilled water, dried in air and mounted in immersion oil and then viewed using bright field mode. Pectin stains red.

2.3 Scanning Electron Microscopy

2.3.1 Freeze Fracture

Seed sections collected as described in Section 2.2 were fixed in FAA fixative over 24 hours at room temperature. After fixation, the seed sections were dehydrated in an ethanol series as described in section 2.2.1. Then the sections were immersed in liquid N_2, broken into small fragments by a stainless steel knife, and stored in absolute EtOH for 1 hour. All the fragments were critical point dried, mounted on a metal stub, and gold-coated using a "Hummer V" Gold Sputter Coater machine.

2.3.2 Observations for Scanning Electron Microscopy

Seed fragments (as described in Section 2.3.1) were scanned using Philips XL 30 Environmental Scanning Electron Microscope (ESEM) (Koninklijke Philips Electronics N.V. Eindhoven, Netherlands) under conventional SEM mode. All SEM images were taken using a CCD digital camera, and saved in the computer directly.

2.4 Transmission Electron Microscopy

2.4.1 Sample Preparation for TEM

Fresh seed segments (as described in Section 2.2) were cut into strips (0.5~1mm X 1-2 mm) under water in a Petri dish to exclude air at cut face. The sections were put into microcentrifuge tubes, filled with 600µl fixative solution (4% paraformaldehyde, 0.8 % glutaraldehyde, and 0.1M KH_2PO_4 buffer pH 7.2) with 10µl Tween 20, placed in the microcentrifuge tube holder and placed into the Pelco BioWave ^{TM} 34700 Laboratory Microwave System (Ted Pella, Inc., Redding, CA, USA). All fixation, dehydration and

embedding steps were performed in the Laboratory Microwave System (http://www.proscitech.com.au/catalogue/notes/pelmicrovac.htm).

2.4.1.1 Aldehyde Fixation

The starting temperature of the fixative was lowered to <20°C by ice. A vacuum of 500 torr (20" Hg) was drawn in The Microwave System set to 250 W and 37°C. The microwave was then programmed for the following time sequences (2X):

1) 1 minute at 0% power;

2) 40 seconds at 100% power;

3) 3 minutes at 0% power.

2.4.1.2 Buffer Rinse

At the end of the 3 minute 0% power sequence, the vacuum was released. The fixative was removed using pipettes and the samples washed twice with 0.1M KH_2PO_4 buffer, pH7.2. The samples were placed back in the microwave under vacuum (500 torr), the system set to 250 W and 40°C, and microwaved for the following intervals (2X):

1) 1 minute at 0% power

2) 40 seconds at 100% power

2.4.1.3 Osmium Fixation

Following the buffer rinse, 600µl of osmium fixative (1%, cooled to <20°C) was added. The system was set to 250 W and 37°C. The microwave was then programmed for the following time sequences:

1) 1 minute at 0% power

2) 40 seconds at 100% power

3) 3 minutes at 0% power

At the end of the sequence, the osmium fixative was removed from the samples (in the fume hood) and the tissue rinsed with tap water prior to transfer to flow-through baskets for dehydration (Giberson et al., 1997) and resin infiltration.

2.4.1.4 Dehydration

The system was set to 250 W and 37°C. The dehydration schedule was as follows: 1 x 30% ethanol; 1 x 50% ethanol; 1 x 70% ethanol; 1 x 80% ethanol; 1 x 90% ethanol; 1 x 95% ethanol and 2 x 100% ethanol. Each dehydration step lasted 40 seconds at 100% power.

2.4.1.5 Vacuum Resin Infiltration

The dehydrated tissues were transferred to acetone and microwaved twice at 250 W and 37°C followed by 40 seconds at 100% power. The tissues were then ready for vacuum resin infiltration.

In this work, samples were infiltrated and embedded in JEMBED resin for TEM. The formulation used was 10 mL JEMBED, 7 mL Nadic Methyl Anhydride, 8 mL Dodecenyl Succinic Anhydride, and 0.4 mL DMP-30(all chemicals from J.B. EM Services, Pointe Claire, PQ). Conditions were set to 450 W and 43°C, and a vacuum of 500 torr was applied. Three two minute vacuum infiltration steps were performed in the microwave (100% resin was used for each infiltration step). Fresh resin was used for each step. After the last two minute run, the tissue was placed in capsules for polymerization.

2.4.1.6 Polymerization

The embedding capsules were filled with resin, covered by their caps and polymerized under water in the microwave. The system was set to 750 W. The microwave was then programmed for the following time sequences:

1) 10 minutes at 60°C

2) 10 minutes at 70°C

3) 10 minutes at 80°C

4) 40 minutes at 100°C

(Water was added as needed to maintain a level above that of the embedding capsules)

2.4.2 Sectioning for TEM

Ultra-thin sections (~10 nm) were cut using a Diatome, ultra 45 ° diamonds knife (Diatome-U.S., Hatfield, PA, U.S.A.) on a Reichert-Jung Ultracut E microtome (Reichert-Jung Optische Werke AG, Wien, Austria), picked up with a single hole Chien grid (Electron Microscopy Sciences, Hatfield, PA) and transferred to a nitrocellulose-carbon coated 300 mesh nickel grid. First, the sections were stained with uranyl acetate (5%) for 15 min in the dark followed by washing with fresh distilled water (1 min). Second, sections were stained with lead citrate for 5min, followed by washing with fresh distilled water (1 min). The grids with stained sections were air dried before TEM observation.

2.4.3 Ultrastructural Observations for TEM

Ultra-thin sections were examined in a Zeiss EM902 transmission electron microscope (Zeiss, Germany) at 80 kV. Sections were imaged on Kodak 4489 Estar thick base Electron Microscope Films (Eastman Kodak Company, Rochester, NY, U.S.A.). Image-

plates were developed in Kodak D19 developer (diluting stock solution 1:2) for 4 min, rinsed in water for 1 min, and fixed in Kodak Rapid fixer for 3 min. After washing in water for 30 min and drying in a dust-free cabinet, the images were scanned to a computer with an Epson Perfection 4870 Photo Scanner (SEIKO EPSON CORP., Japan).

2.5 Confocal Microscopy

2.5.1 Sample Preparation for Confocal Microscopy

Fresh soybean seeds (as described in Section 2.1) were cut into 8 μm sections in phosphate buffer and saline solutions (PBS, 0.01M, pH 7.2) using a razor blade on a Microslicer® DTK-1000 microtome (D.S.K., Kyoto, Japan). The sections were stained immediately. In this work, two different dyes were used: Neutral Red and Chloronaphthol.

2.5.1.1 Neutral Red

Neutral Red (0.01% in 0.6M KNO_3, 1mM $CaCl_2$, and KH_2PO_4 buffer, pH 7.5) was used for observing the vacuoles in soybean seeds. Slides were stained in the dark for 3 min, mounted in 50% glycerol and then viewed. Emission of Neutral Red signals was imaged at 515-575 nm using a 532 nm laser.

2.5.1.2 Chloronaphthol

Chloronaphthol was used for observing the peroxidase in soybean seed coats. Chloronaphthol staining solution was prepared by adding 0.5 ml of 4-chloro-1-naphthol (30 mg ml^{-1} in absolute ethanol) and 0.3 ml of 30% H_2O_2 to 50 ml of PBS (0.01M, pH 7.2) (Gijzen et al. 1993). Slides were stained in the dark for 3 min, mounted in 50% glycerol and

then viewed with the confocal microscope (excitation at 450nm, signal imaging using a slit setting of 420-515nm).

2.5.2 Confocal Microscopy Processing

The stained sections were examined in a Zeiss LSM 510 META confocal microscope (Zeiss, Germany). All images were obtained by a CCD digital camera.

2.6 Immunogold Labelling in Transmission Electron Microscopy

2.6.1 Sample Preparation

Fresh seed pieces (as described in Section 2.1) were cut into strips (0.5~1mm X 1-2 mm) in water in a Petri dish to exclude air at cut face. Conditions for aldehyde fixation were as outlined in Section 2.4.1.1

Following aldehyde fixation, the samples were rinsed with tap water prior to transferring them to the flow-through baskets for dehydration (Giberson et al., 1997) and resin infiltration.

Dehydration conditions were as outlined in section 2.4.1.4

2.6.1.1 Vacuum Resin Infiltration

The Laboratory Microwave System was setup as in Section 2.4.1.6.

LR White (London Resin Company, Reading, UK) was used for resin infiltration. The temperature restriction was set to 450 W and 43°C, and under a vacuum (20" Hg; 500 torr). Three two minute vacuum infiltration steps were done in the microwave (100% L.R. White was used for each infiltration step). Fresh LR White was used for each step. After the last two minutes, the tissue was placed in capsules for polymerization.

2.6.1.2 Polymerization

The embedding capsules were filled with LR White, covered by their caps and polymerized in a conventional oven at 55°C for 20 hours.

2.6.2 Sample Preparation for Immunogold Labelling in TEM

Ultra-thin sections (~10 nm) were cut by a Diatome ultra 45° diamond knife (Diatome-U.S., Hatfield, PA, U.S.A.) using a Reichert-Jung Ultracut E microtome (Reichert-Jung Optische Werke AG, Wien, Austria) and picked up with a Chien grid and transferred to a nitrocellulose-carbon coated 300 mesh nickel grid. The grids were stored for immunohistochemistry at a later date.

2.6.2.1 The Immunogold Reaction

The nickel grids were placed, with section-side down, on a drop of 1% glycine in PBS (0.01M, pH 7.2) in a plastic Petri dish for 30 min to block free aldehydes. After washing with PBS (3X 5min), the grids were then incubated with 1% ovalbumin for 10 min to minimize non-specific binding, then transferred directly to the primary antibody diluted 1:400 in 0.1M PBS+ 0.1% ovalbumin (PBSO). The Petri dish was incubated in a humid chamber at 4°C overnight. A control was performed under the same conditions without the primary antibody. Both groups of grids were then washed 3X 5 min, then re-blocked with 1% ovalbumin for 10 min. The sections were then transferred to goat anti-rabbit IgG conjugated to 15nm gold particles (E-Y Laboratories, San Mateo, CA) diluted 1:20 in the PBSO for 1 hr at room temperature (using the supernatant after a centrifugation at 500xg for 10 min). After three washes in PBS and two washes in distilled H_2O, each for 5 min, the

sections were fixed with 4% glutaraldehyde for 20 min, washed with PBS 3X 5 min, stained with uranyl acetate in the dark for 15 min, followed by washing with water for 1 min, and stained with lead citrate for 5min, followed by washing with fresh distilled water 1 min. The sections had been kept wet until this point. Grids were dried on a filter paper before transferring to a silicon pad in a Petri dish.

The primary antibody was rabbit anti-SBP, a gift from M. C. Romero (Southern Crop Protection and Food Research Centre, Agriculture and Agri-Food Canada , London , ON , Canada). The sensitivity of this antibody was tested by Western blot analysis using a colorimetic assay (Invitrogen, ELF, catalogue number N6547). Based upon unpublished work (M.C. Romero, J. Schnell) the antibody can detect 10 ng of partially purified SBP (Sigma, catalogue number P14232). It does not detect SBP in extracts of seed coats isolated from cv Jack but does in extracts of seed coats from cv Harosoy63.

2.6.3 Ultrastructural Observations for TEM

Ultra-thin sections were examined at 80 kV with a Zeiss EM902 transmission electron microscope (Zeiss, Germany) and images obtained as described in Section 2.4.3.

CHAPTER THREE: RESULTS

3.1 Differentiation of Hour Glass Cells in the Soybean Seed Coat

During the early stages of hour glass cell (HGC) development in soybean seed coats, HGCs start to differentiate at 12 dpa, beginning with cells of the hypodermis near the top or hilum portion of the seed (see Figure 6 of Miller et al., 1999). Between 12 and 15 dpa, HGCs complete most of their transformation - their cell shape changes dramatically, thickened cell walls appear and starch granules are observed (Miller et al., 1999).

In this thesis we have used several microscopy techniques including light microscopy (LM), transmission electron microscopy (TEM), scanning electron microscopy (SEM) and confocal microscopy (CM) to investigate the development of the HGC within the seed coat with emphasis on this crucial time period. These studies mainly focused on soybean cvs Maple Presto, Harosoy63 and Jack. Jack is a cultivar used for transformation to create genetically modified seed coats. The LM study of HGC differentiation employed Jack; Maple Presto was used for TEM and SEM studies of HGC development; and both Jack and Harosoy63 were used for confocal microscopy.

3.2 Light Microscopy Studies of Developing Seed Coats

Toluidine Blue O and Ruthenium Red were chosen as the two main dyes in this work. Both stain cell walls and can be used to monitor changes during HGC differentiation. Soybean cv Jack was used in this work. All HGCs observed in this section are at the bottom of the seed opposite the hilum. Comparisons of the results presented in this thesis to those of Miller et al. (1999), who studied cv. Maple Presto, will help to confirm the previous results and to generalize them to other soybean cultivars.

At 13 dpa, the HGCs continue to align vertically under the palisade cells and to enlarge, although their cell shape has changed little from 12 dpa (refer to data from Miller et al. 1999 reproduced in Fig.1.2). All cell types- HGC, palisade and parenchyma- appear to be in close contact. The cell walls of the HGC are starting to become thicker but as yet there are no apparent gaps or air spaces between them, and the central vacuole in each HGC is enlarging (Fig. 3.1 A, Fig. 3.2A). Although Toluidine Blue O and Ruthenium Red do not stain starch grains, these grains can be recognized by their size, shape and quantity in HGCs. Starch grains are visible in the HGCs and palisade cells most clearly following staining with Ruthenium Red (Fig. 3.2).

At 14 dpa, the HGCs are continuing to change shape. Their cell walls are thicker, especially at the middle part of the cell, they are assuming the typical hourglass shape, and are increasing in size. Distinct intercellular spaces appear between HGCs. The central vacuole in each HGC continues to expand with cell shape changes and occupies more of cell interior (Fig. 3.1 B, Fig. 3.2B). More starch grains are visible in the palisade cells, hourglass cells and parenchyma cells (Fig. 3.2B).

By 15 dpa, the HGCs have assumed a typical hourglass shape: they are wider at the top and bottom and narrower in the middle. The cell walls are thicker at the sides and thinner at the top and bottom of the cell. The central vacuole occupies most of the HGC and appears "empty". The connections between HGCs and palisade cells are still close; however, the connections between HGCs and parenchyma cells are loose such that the cells appear separated. Although the air spaces among HGCs are clear at this stage, the HGCs continue to remain in contact at the top and bottom. Starch grains are visible in the palisade layer, hourglass cells and parenchyma layer (Fig. 3.1C) especially within the cytoplasm of HGCs, and the vacuoles appear empty (Fig. 3.2C). The colour of the cell walls in sections stained with Toluidine Blue O changed from blue to purple as the

thickness of the cell wall increased (Fig. 3.1). Toluidine Blue O is a cationic thiazine dye (Green, 1990), with metachromatic properties that reflect differences in chemistry of the structures where it binds. Where charged anionic groups in the substrate are close together, the dye molecules are aligned such that dye polymers are formed resulting in a purple to magenta colour, in contrast to the bound monomer form, which is blue (Flint 1994). Thus, the change from blue to purple suggests the presence of large numbers of anionic groups in the wall, which is characteristic of polygalacturonic acid, or pectin.

We have also used these LM pictures to estimate the dimensions of a typical HGC (n = 7 - 10) during this time period. While sample preparation may affect the shape of the cells, all samples were prepared in the same manner giving us a basis for comparison. The width as measured in the middle of the cell increases from 14.1 to 16.0μm from 13 to 15dpa. These values are not significantly different. The width as measured at the top of the cell increases from 14.3 to 20.3μm between 13 and 15dpa while the height increased from 37.2 to 61.2μm during the same time. Thus during the time period from 13 to 15 dpa, HGCs increased their height more than their width. As can be seen in Figure 3.1C, some cells have the hourglass shape while others do not.

These results confirm those of Miller et al. (1999) and provide more detail during the rapid changes that occur from 13-15 dpa. During this time the HGCs enlarge and dramatically change their shape to hourglass shape. This study also confirms that the changes are very similar for the two cultivars, cv Maple Presto (Miller at al., 1999) and cv Jack.

Figure 3.1 Light Micrographs of Hourglass Cells Stained with Toluidine Blue at 13, 14 and 15 Days Post Anthesis

Paraffin sections of hourglass cells stained with Toluidine Blue O prepared as described in Section 2.2.2.1 of Materials and Methods. (A) Cross section of hourglass cells 13 dpa. (B) Cross section of hourglass cells 14 dpa. (C) Cross section of hourglass cells 15 dpa. P, palisade layer; H, hourglass cells; Pa, parenchyma; CW, cell wall; V, vacuole; s, starch grain; as, air space. Bar = 10μm. These examples represent the results from 2 independent experiments with a minimum of 4 micrographs analysed for each time point.

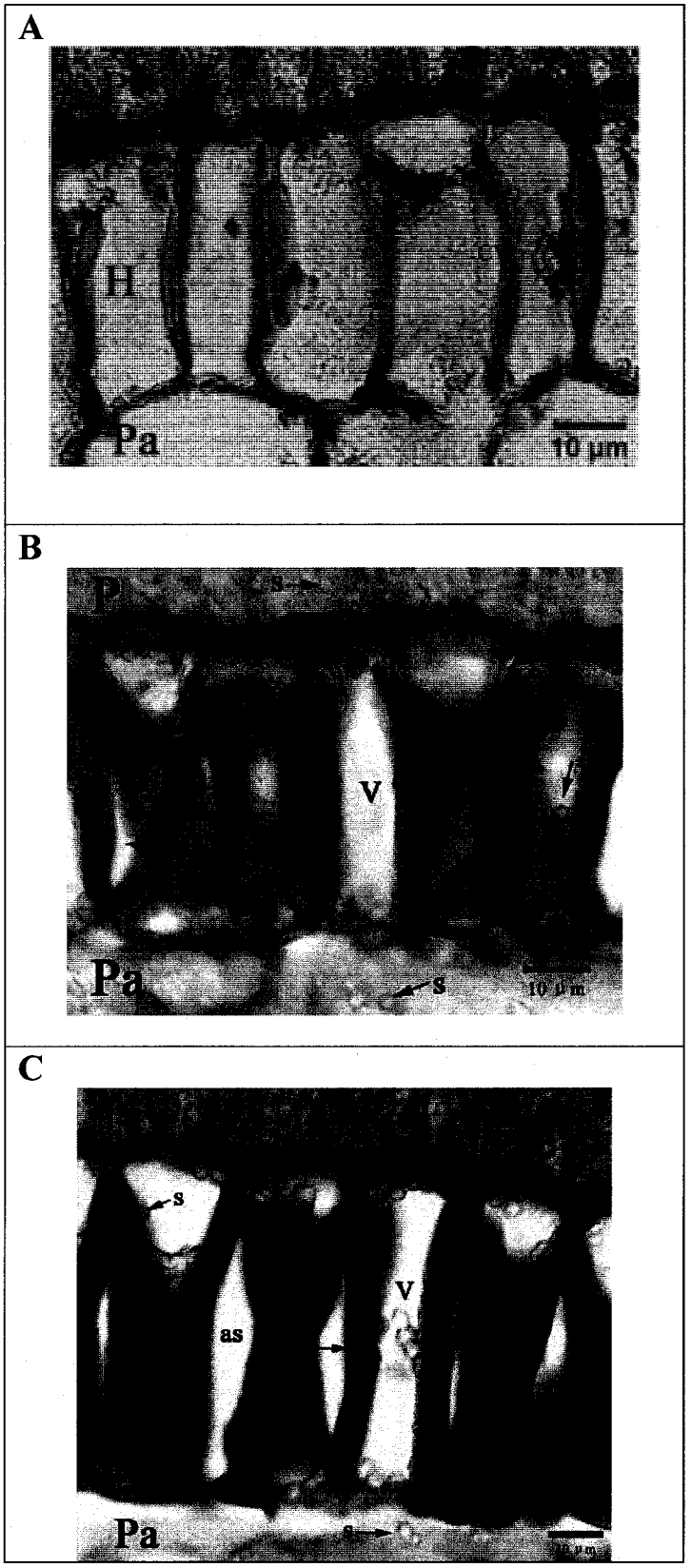
A
H
Pa
10 µm
B
P
s
V
Pa
s
C
s
as
V
Pa
s

Figure 3.2 Light Micrographs of Hourglass Cells Stained with Ruthenium Red at 13, 14 and 15 Days Post Anthesis

Paraffin sections of hourglass cells stained with Ruthenium Red prepared as described in Section 2.2.2.2 of Materials and Methods. (A) Cross section of hourglass cells 13 dpa. (B) Cross section of hourglass cells 14 dpa. (C) Cross section of hourglass cells 15 dpa. P, palisade layer; H, hourglass cells; Pa, parenchyma; CW, cell wall; N, nucleus; V, vacuole; s, starch grain; as, air space. Bar = 10μm. These examples represent the results from 2 independent experiments with a minimum of 4 micrographs analysed for each time point.

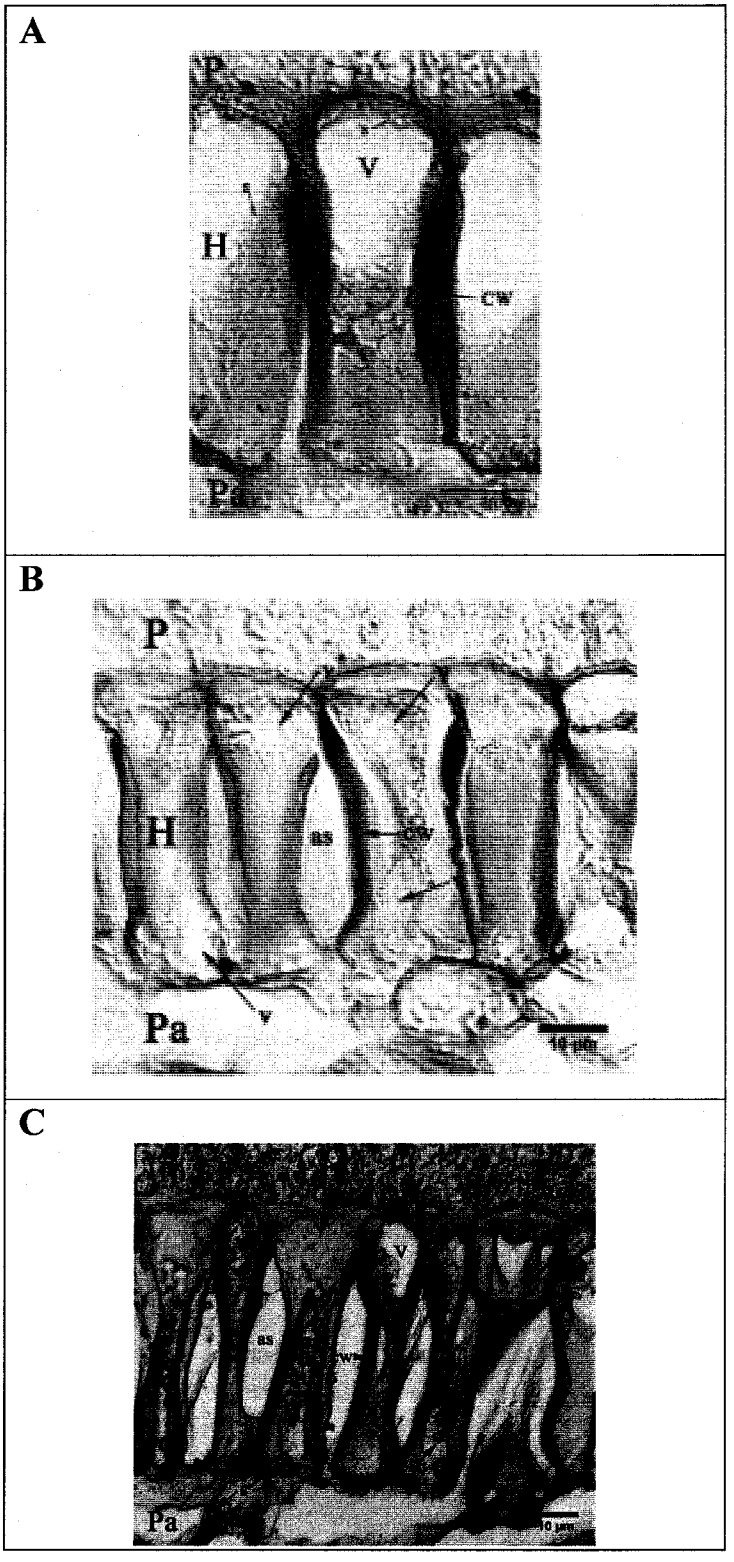
A
P
V
H
CW
Pa
B
P
H
as
cw
v
Pa
10 µm
C
V
as
cw
Pa
10 µm

3.3 Analysis of HGC Ultrastructure during Soybean Seed Coat Development by TEM

In this study, fixed, resin-embedded soybean seed coat material was cut into ultra thin sections (~10 nm) and observed using TEM. This technique is useful for observing cell ultrastructure and endomembrane systems, and offers the advantages of very high magnification and high resolution images.

To compare with Miller's work (1999), the same soybean cultivar (Maple Presto) was used. Nine different stages, 9 dpa, 12 dpa, 15 dpa, 18 dpa, 21 dpa, 24 dpa, 27dpa, 30 dpa and 45 dpa, were examined during soybean seed coat development. All HGCs observed in this section were taken from section at the bottom of the seed in the cells opposite the hilum.

3.3.1 Nine Days Post Anthesis

At 9 dpa, the seed begins to enlarge. Most hypodermis cells show the rectangular cell shape (Fig 3.3). The hypodermis cells are arranged tidily. The adjoining cell walls touch each other without any intercellular air spaces. Compared with the small intercellular spaces between parenchyma cells and hypodermis cells, there are some obvious large air spaces between hypodermis cells and palisade cells. As the cell is relatively small the nucleus appears relatively large. The circular nucleus has a smooth surface with a high density nucleolus. Condensed chromatin is visible (Fig 3.3B) just inside the nuclear membrane. The cytoplasm contains numerous Golgi, ER, proplastids and mitochondria (Fig. 3.3B). Some chloroplasts which contain large starch grains are shown in the cells. The HGC wall is not symmetrical, being thin in the middle and thick on the top and bottom of the cell. Plasmodesmata can be observed linking the HGCs. There is a large vacuole near the nucleus, which occupies approx. 40% of the cell.

3.3.2 Twelve Days Post Anthesis

At 12 dpa, the hypodermis is starting to differentiate into hourglass cells (Fig 3.3C). HGCs become much thinner and longer. The central vacuole occupies most of the cell. As a result the nucleus and cytoplasm are confined to the remaining thin layer between the plasma membrane and the tonoplast. Most connections between HGCs are still close, although a few small air spaces are formed at cell corners. The cell walls at the bottom of the palisade cells become much thicker than those at 9 dpa. Compared with the firm connection between the palisade cells and HGCs, the connection between parenchyma cells and HGCs is weak and easily separated. The dense cytoplasm of HGCs contains several mitochondria, ER, proplastids, Golgi and chloroplasts with starch grains. The central vacuole is not as small as that at 9dpa. Various multiform vacuolar inclusions, which are the waste products from cell metabolism, are found in the central vacuole. There are no starch grains in the central vacuole. The cell wall of HGC is still a single thin layer and there are no clear differences compared with the cell walls at 9 dpa. Plasmodesmata can be visualized (described later, see Section 3.4 and Fig 3.5).

3.3.3 Fifteen Days Post Anthesis

At 15 dpa, HGCs have completed most of their transformation and have become highly vacuolar, thick walled cells. During their extension, HGCs have changed to the final hourglass shape. In spite of the shrinking of HGCs in the middle leading to large air spaces between cells, the top and bottom parts of HGCs remain closely connected. One large central vacuole still occupies most of the cell. The nucleus and cytoplasm are compressed in the remaining space in the lumen. In addition to changes in the cell shape, the cell wall has undergone a dramatic developmental change. The secondary cell wall of

the hourglass cell becomes thicker as a result of deposition of extra wall layers, a process that continues as the seed develops. The thickest part of the cell wall approaches 7.4μm. There are more layers in the middle of the HGC and fewer towards the top and bottom of the cells. The cytoplasm has high density because of the increasing starch grains, and contains several mitochondria, ER, Golgi and proplastids. A large vacuolar inclusion, which is considered proteinaceous, appears in the central vacuole (Fig. 3.3D).

3.3.4 Eighteen Days Post Anthesis

At 18 dpa, the hourglass cells are well defined and have attained their classic shape. HGCs are separated at their mid points by large air spaces, but their top and bottom cell walls still adjoin closely. Compared with the relatively weak link between HGCs and parenchyma cells, the palisade cells and HGCs still have a strong connection. The cell walls of HGCs are much stronger than the cell walls of palisade cells and parenchyma cells as a result of much reinforcement. The cell walls in the middle continue to thicken with more layers being added in comparison to 15dpa but the cell walls at the tops and bottoms, while thickening, are much thinner than in the middle. The central vacuole expands in volume with increasing cell size. The cell accumulates and stores abundant large inclusions in the central vacuole. The vacuolar inclusions show different densities, and are found mainly in the top and bottom part of the HGC. The cytoplasm, which contains few starch grains, occupies a low proportion of the cell. It adheres to the cell wall because of the pressure from the central vacuole (Fig. 3.3E). Many starch grains are stored in the palisade at this stage. HGCs have smooth inner cell wall surface and fewer starch grains. The tonoplast is clearly visible surrounding the vacuole, which contains abundant vacuolar inclusions at this stage. Vacuolar inclusions are found in palisade cells also (Fig. 3.3F).

3.3.5 Twenty One Days Post Anthesis

At 21 dpa, the thick cell wall of HGCs shows many layers (Fig 3.3G). Large air spaces are visible between HGCs. The cell walls and cell shapes of the HGCs do not change much, in contrast with the ultrastructure of the cells. Although the central vacuole still occupies most of the HGC, the content of vacuolar inclusions is much less than at 18 dpa. The cell membrane is observed clearly attaching with the cell wall, but the tonoplast of the central vacuole begins to deteriorate. The cytoplasm, with the lower density, contains many chloroplasts and Golgi. A few small electron opaque vesicles, which could be protein storage vesicles, are found in the cytoplasm of both HGCs and parenchyma cells. A lot of starch grains are stored in the palisade cells, but no clear starch grains are found in HGCs and parenchyma cells.

3.3.6 Twenty Four Days Post Anthesis

At 24 dpa, the ultrastructure of HGCs enters a new stage (Fig. 3.3H). The cell membrane of the HGC is very clear, and the tonoplast continues to degrade. The vacuolar contents are starting to mix with cytoplasm. The HGC contains a single nucleus, and many mitochondria and chloroplasts. The vacuolar inclusions are continuing to degrade in the cell, as shown by loss in their density and volume.

3.3.7 Twenty Seven Days Post Anthesis

At 27 dpa, the ultrastructure of HGCs does not change from that at 24 dpa. The cytoplasm and the central vacuole contents have fused together, so it is hard to tell them individually within the cell. The HGC contains a single nucleus, many ER, Golgi, chloroplasts and a few vacuolar inclusions. The cell wall has become smooth and its

layers are less distinct. The palisade cells store many starch grains, but there are no starch grains in the HGCs. (Fig. 3.3I)

3.3.8 Thirty Days Post Anthesis

At 30 dpa, the ultrastructure of HGCs is unchanged. The HGC contains many ER, Golgi, chloroplasts and vacuolar inclusions. The cell membrane is very distinct.

3.3.9 Forty Five Days Post Anthesis

At 45 dpa, the HGCs are fully mature and their ultrastructure has changed. Most organelles are degraded, and their remnants fill the vacuole. The cell membrane is very clear, as are the multiple layers of the thick cell wall. Although the nucleus is still in the vacuole, its nucleolus and chromatin are disappearing, so its density is very low (Fig 3.3L).

From 9 dpa to 30 dpa, HGCs undergo dramatic changes from a single thin cell walled hypodermis cell to an hourglass shaped cell surrounded by a thick multi-layered cell wall. The central vacuole of HGC always enlarges following cell wall extension. Vacuolar inclusions first appear at 15 dpa, and then degrade after 21 dpa. By 45 dpa, all organelles in HGCs have been degraded, and their remnants fill the whole central vacuole.

These results confirm the work of Miller et al. (1999) and add much new information on cell ultrastructure during HGC development. During soybean seed coat development, the HGCs enlarge and dramatically change their shape to hourglass shape, increase the thickness of their cell walls, show obvious intercellular air spaces and extend their central vacuoles.

Figure 3.3 Transmission Electron Micrographs of Developing Hourglass Cells

Samples were taken at the times indicated and processed as described in Materials and Methods Section 2.4. (A) Micrograph of hourglass cells at 9 dpa. (B) Micrograph of hourglass cells at 9 dpa at higher magnification. (C) Micrograph of hourglass cells at 12 dpa. (D)Micrograph of hourglass cells at 15 dpa. (E) Micrograph of hourglass cells at 18 dpa. (F) Micrograph of hourglass cells at18 dpa at higher magnification. (G) Micrograph of hourglass cells at 21 dpa. (H) Micrograph of hourglass cells at 24 dpa. (I) Micrograph of hourglass cells at 27 dpa. (J) Micrographs of hourglass cells at 30dpa. (K) Micrograph of hourglass cells at 45 dpa. (L) Micrograph of hourglass cells at 45 dpa at a higher magnification showing the nuclear region. These examples represent 2 independent experiments. A minimum of 2 micrographs were analysed for each time point.

as, air space; C, chloroplast; ch, chromatin; CM, cell membrane; CW, cell wall; CY, cytoplasm; ER, endoplasmic reticulum; Hp, hypodermal cells; G, Golgi apparatus; M, mitochondrion; N, nucleus; NL, nucleolus: NM, nuclear membrane, pl, plasmodesmata; P, palisade layer; PA, parenchyma cells; PP, proplastid; S, starch grain; SV, small electron opaque vesicle; t, tonoplast; V, vacuole; i, vacuolar inclusion.

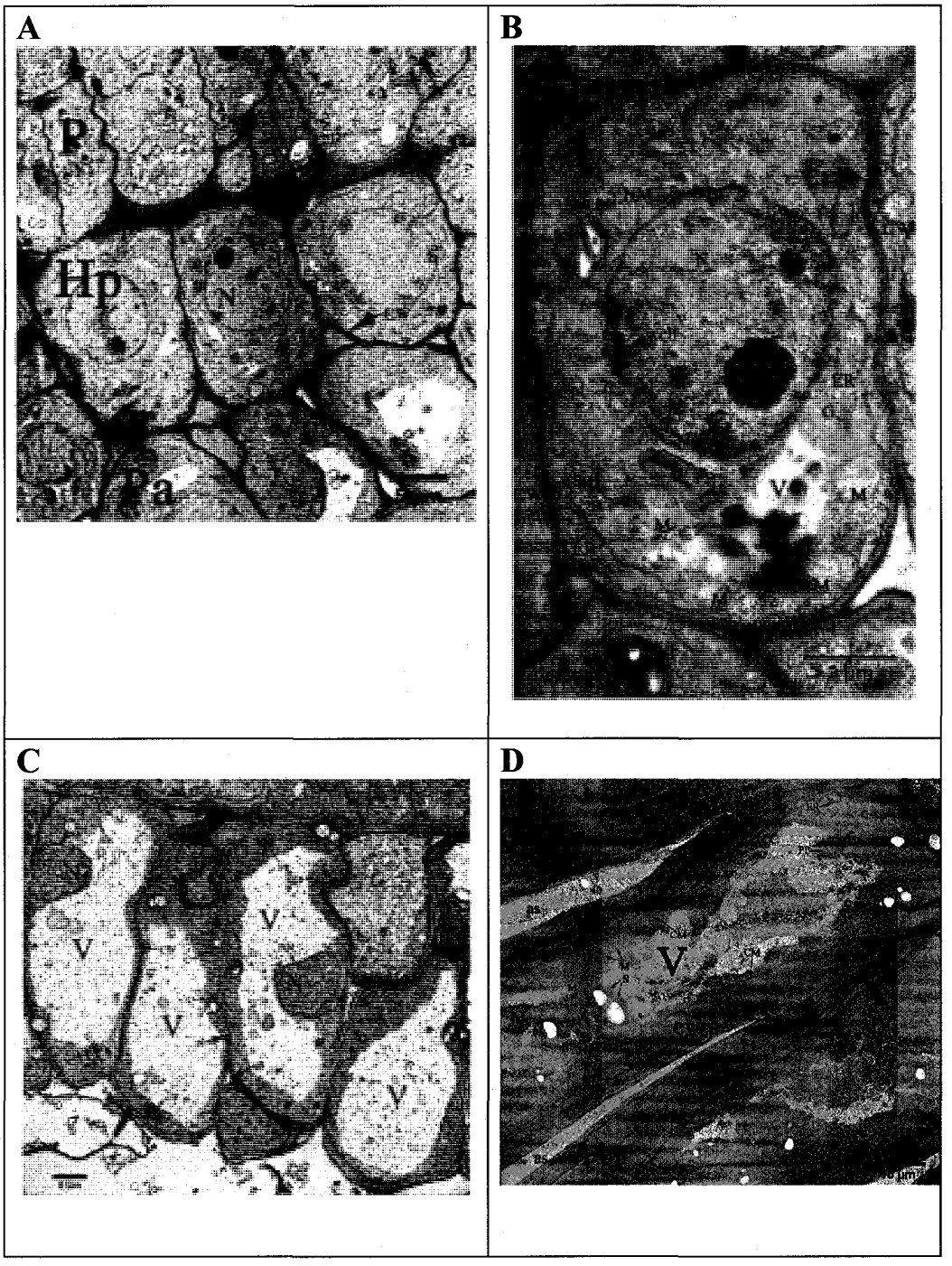
A
P
Hp
N
Pa
B
C
V
V
V
V
D
V

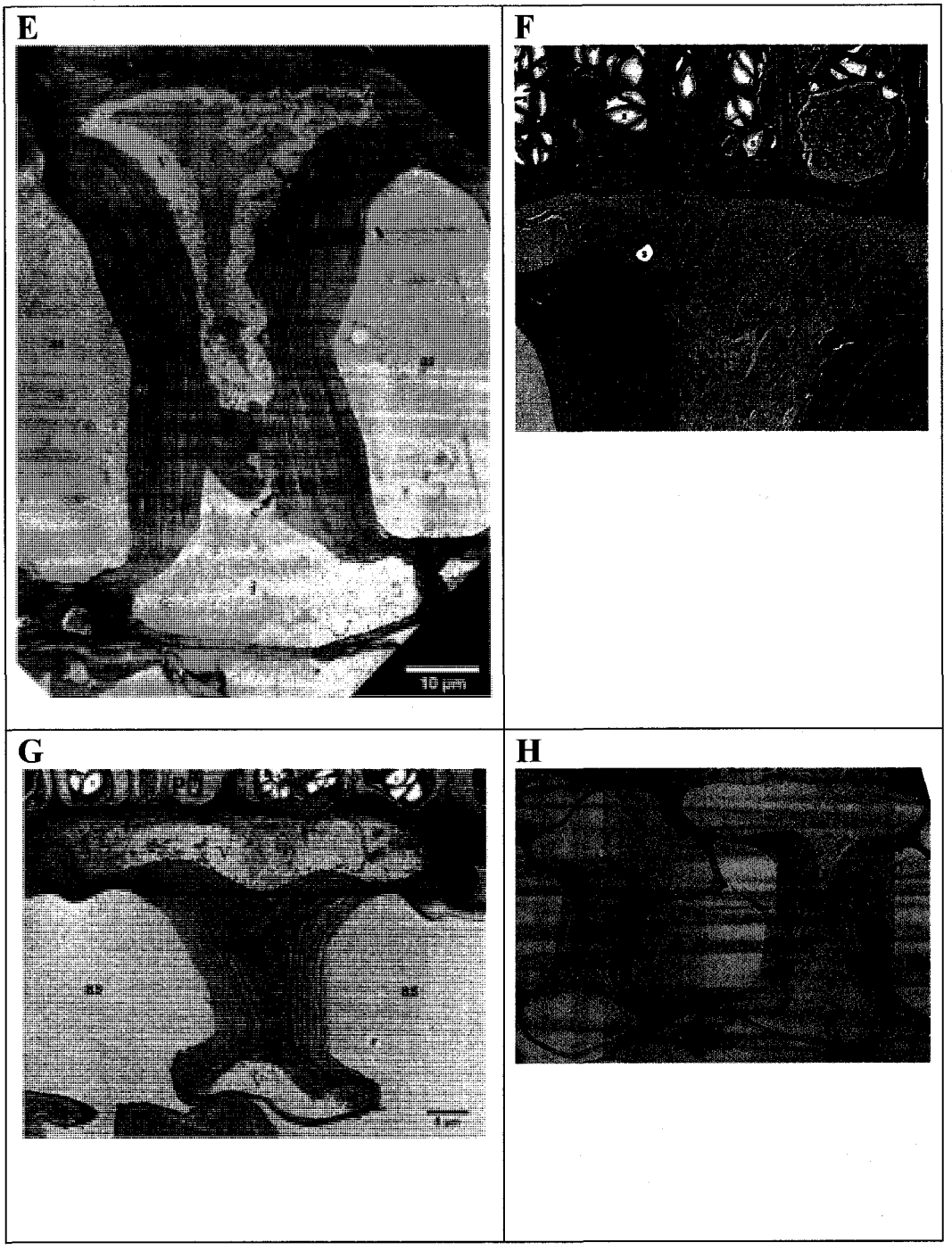
E
F
G
H

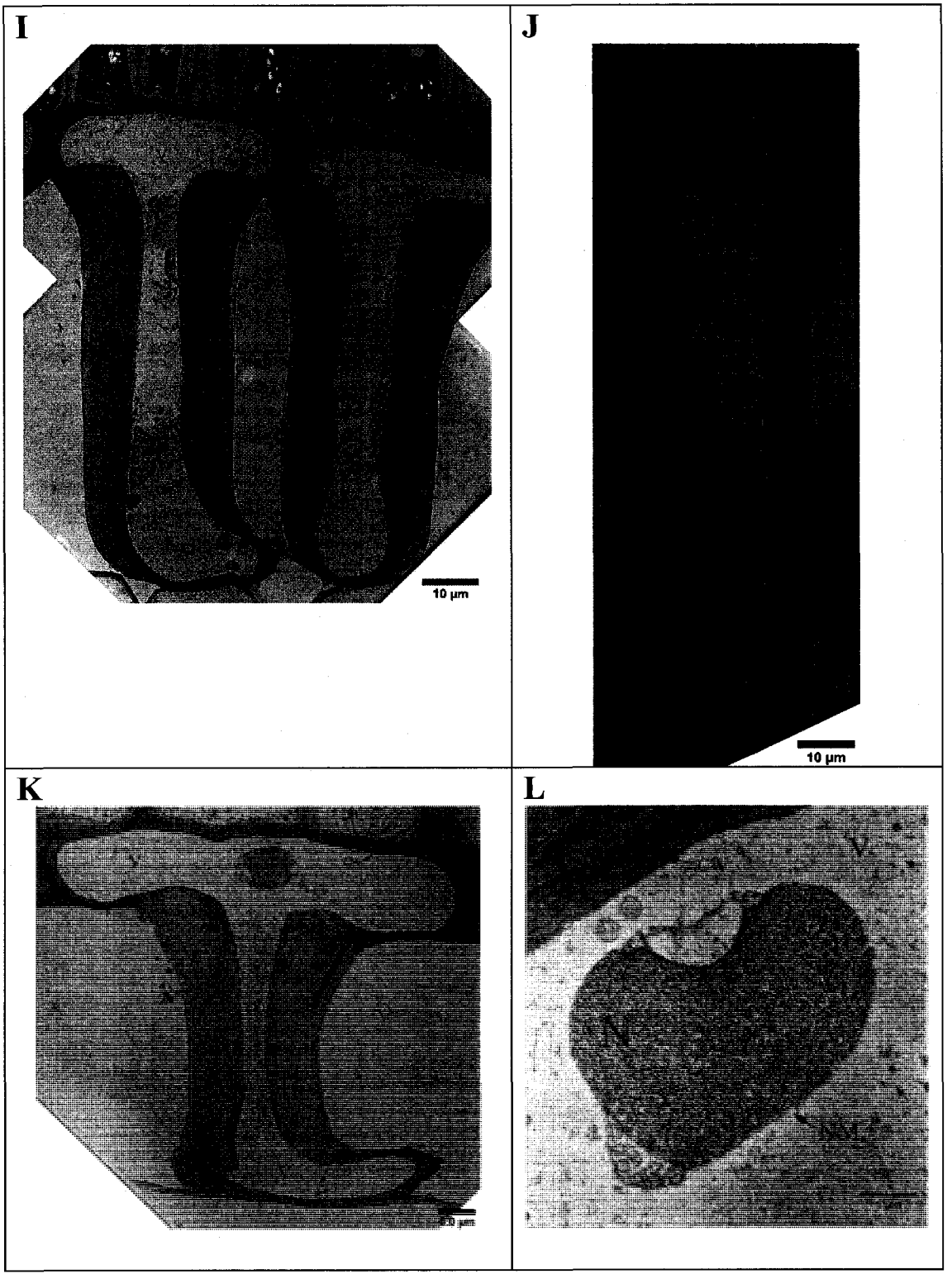
I
10 µm
J
10 µm
K
L

3.4 SEM Examination of HGCs during Soybean Seed Coat Development

In this work, freeze fractured fragments of the soybean seed coat were observed using SEM. To compare with Miller's work (1999), the same soybean cultivar (Maple Presto) was used. Nine different stages, 9 dpa, 12 dpa, 15 dpa and 18 dpa were examined during soybean seed coat development. All HGCs observed in this section are at the bottom of the seed in the cells opposite the hilum.

Compared with TEM work, the SEM work showed us less information of ultrastructure of HGCs during soybean seed coat development. However, the SEM work showed some physical features of HGC development, which TEM could not do.

3.4.1 Nine Days Post Anthesis

At 9 dpa, the cells of the hypodermis showed a cuboidal cell shape with thin and weak cell walls. There were no air spaces between HGCs. A central vacuole occupied approx. 40% of the cell (Fig. 3.4A).

3.4.2 Twelve Days Post Anthesis

At 12 dpa, the cells of the hypodermis enlarged in size and showed a long and thin cell shape. Its cell walls were still weak and could be broken. There were no obvious air spaces between HGCs. A central vacuole occupied most room of the cell (Fig. 3.4B).

3.4.3 Fifteen Days Post Anthesis

At 15 dpa, the cells of the hypodermis showed hourglass cell shape (Fig3.4C). Their cell walls were stronger and showed several layers, but they were still breakable during SEM

sample preparation. Many obvious air spaces appeared between HGCs. The central vacuole still occupied most of the cell.

3.4.4 Eighteen Days Post Anthesis

At 18 dpa, HGC showed completely hourglass cell shape (Fig. 3.4D). The middle cell walls of HGCs were too strong to be broken for SEM, so their inner structures could not be observed by SEM. Many obvious large air spaces were visible between HGCs, but the top parts of HGCs connected closely with each other and with the palisade layer.

After 18dpa, further differences were not observed with SEM and micrographs for those time points are not presented. These SEM results complement the TEM results and reconfirm the work of Miller et al. (1999). During soybean seed coat development, the HGCs enlarge and dramatically change their shape to hourglass shape, increase cell wall thickness, develop obvious intercellular air spaces and extend their central vacuoles.

Figure 3.4 SEM work for the ultrastructure of hourglass cells

Samples were taken at the times indicated and processed as described in Materials and Methods Section 2.4. These examples represent 3 independent experiments with a minimum of 3 micrographs analyzed for each time point.

(A) Scanning electron micrograph of hourglass cells at 9 days post anthesis. (B) Scanning electron micrograph of hourglass cells at 12 days post anthesis. (C) Scanning electron micrograph of hourglass cells at 15 days post anthesis. (D) Scanning electron micrograph of hourglass cells at 18 days post anthesis. CW, cell wall; CM, cell membrane; V, vacuole; N, nucleus; P, palisade layer; H, hourglass cells; Pa, parenchyma; cy, cytoplasm; as, air space.

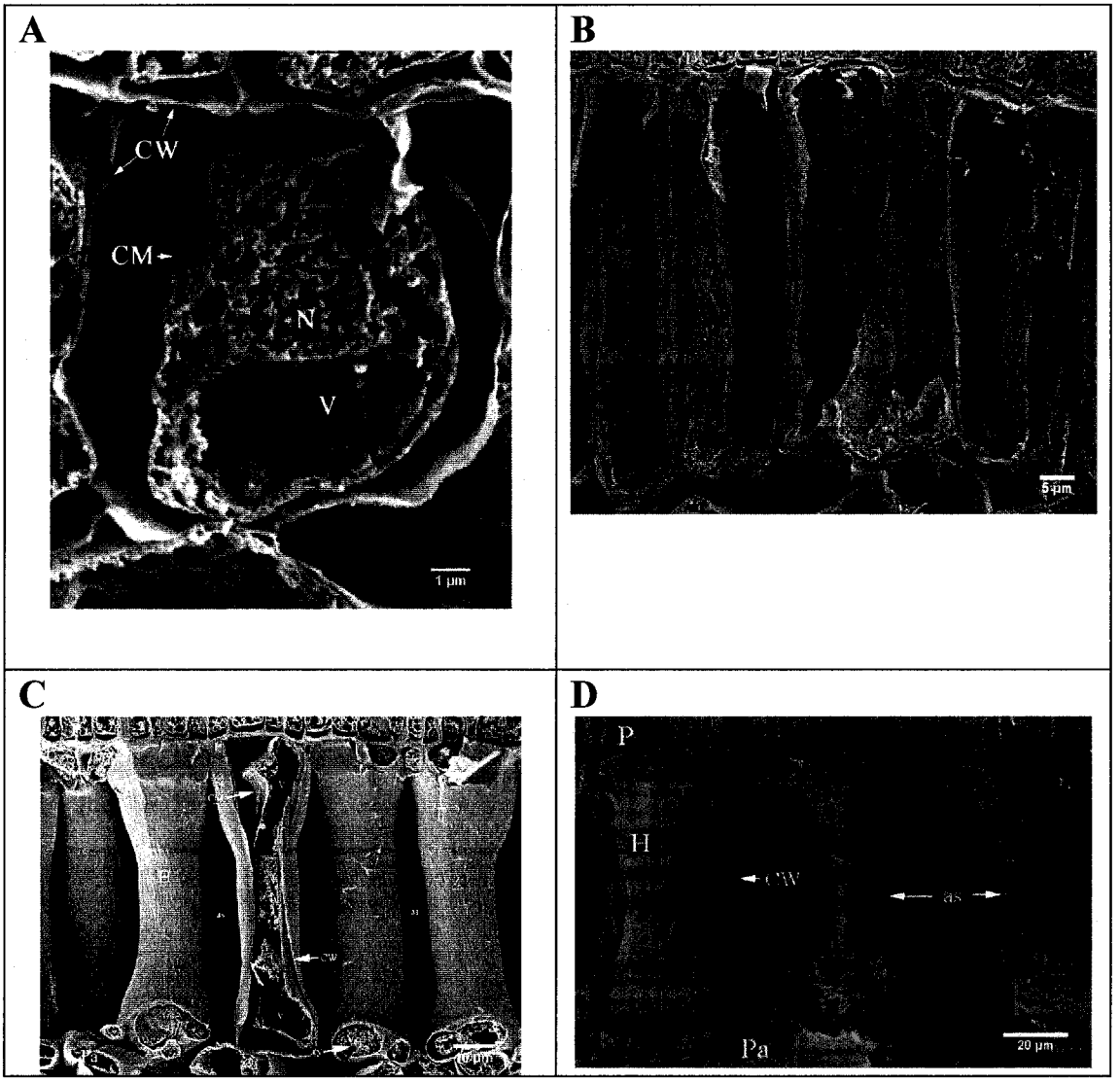
A
CW
CM
N
V
1 µm
B
5 µm
C
D
P
H
CW
as
Pa
20 µm

3.5 Plasmodesmata form bridges between cells in Soybean Seed Coat

As plasma-membrane-lined channels in plant cell walls, plasmodesmata provide passageways for symplastic communication between cells. Plasmodesmata play an important role in plant cells by facilitating the direct intercellular transport of photoassimilates, ions and growth regulators (Heinlein, 2002). The structure of plasmodesmata has been described in Section 1.2.1. In this work, we have observed plasmodesmata in HGCs at different stages during soybean seed coat development.

I observed plasmodesmata between HGCs at 9 dpa (Fig. 3.3.B). At 15 dpa, plasmodesmata were visible between palisade cells (Fig. 3.5A), between palisade cells and HGCs (Fig. 3.5B), between HGCs (Fig. 3.5C), between HGCs and parenchyma cells (Fig. 3.5C and Fig. 3.5D) and between parenchyma cells (Fig. 3.5D). Thus, all cells in soybean seed coats form a web interconnected by plasmodesmata. Plasmodesmata were also found between mature HGCs where they were joined at the base of the cells at 30 dpa (Fig. 3.6A) and 45 dpa (Fig. 3.6B).

Thus, these result show that plasmodesmata connect all three main cell types in the soybean seed coat as early as 15dpa, and exist between HGCs at every stage during seed coat development. The presence of plasmodesmata suggests the capability of transfer of materials between cells exists throughout seed coat development.

Figure 3.5 Plasmodesmata in soybean seed coat

(A) Transmission electron micrograph of palisade cells at 15 days post anthesis. (B) Transmission electron micrograph of hourglass cells at 15 days post anthesis. (C) Transmission electron micrograph of hourglass cells and parenchyma cells at 15 days post anthesis. (D) Transmission electron micrograph of hourglass cells and parenchyma cells at 15 days post anthesis.

Pa, parenchyma cells; P, palisade cells; H, hourglass cells; pl, plasmodesmata.

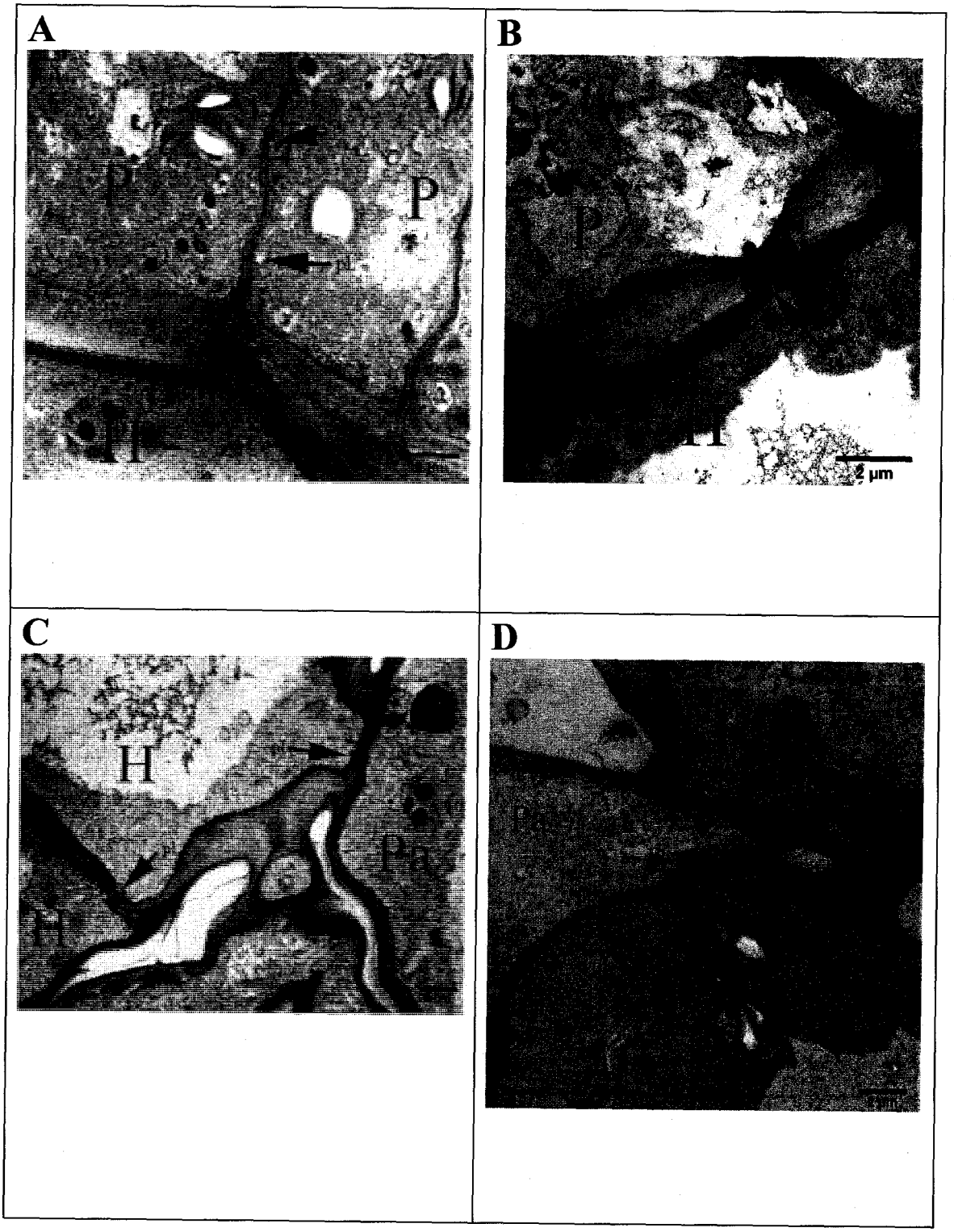
A
P
P
H
B
P
H
2 µm
C
H
P
H
D

Figure 3.6 Plasmodesmata between mature hourglass cells

Plasmodesmata in adjoining cells at the bottom of hourglass layer. (A) Transmission electron micrograph of hourglass cells at 30 days post anthesis. (B) Transmission electron micrograph of hourglass cells at 45 days post anthesis.

H, hourglass cells; CW, cell wall; CM, cell membrane; pl, plasmodesmata; M, mitochondria.

A

B

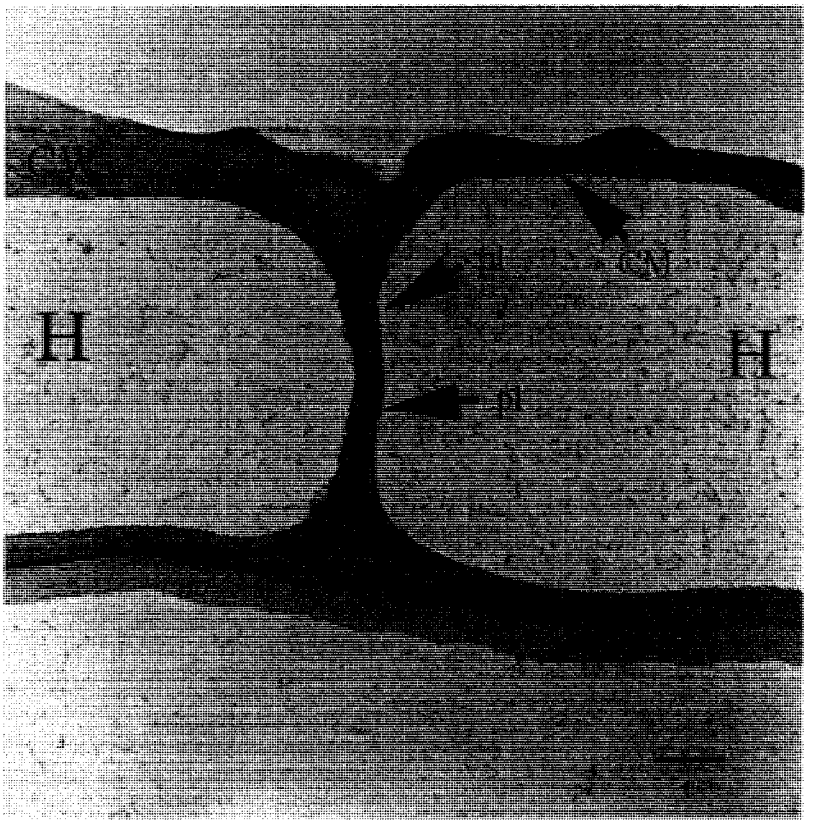

3.6 Peroxidases in HGC Development

In this work, sections of fresh tissues were stained by Chloronaphthol, and observed using a Confocal microscope. Jack seed coat (*epep* cultivar) was expected to give a negative reaction, and Harosoy63 soybean seed coat (*EpEp* cultivar) was expected to give a positive reaction. Three different stages, 12 dpa, 19 dpa, and 30 dpa, were studied during soybean seed coat development.

The content of peroxidases in HGCs changed during development. At 12 dpa (Fig. 3.7), peroxidases were detected in the palisade layers in both positive and negative samples. A few peroxidases apparently bound to starch grains were found the HGCs in Harosoy63 (Fig. 3.7(1)). No peroxidases were detected in the HGCs in Jack (Fig. 3.7(2)). At 19 dpa (Fig. 3.8), both cultivars' palisade layers still contained peroxidases. The HGCs in Harosoy63 had plentiful peroxidases. The peroxidase staining was concentrated in the cytoplasm (Fig. 3.8(1)). In contrast, the HGCs in Jack appeared to have just a small amount of peroxidase staining, but the parenchyma cells below them contained more peroxidase staining (Fig. 3.8(2)). At 30 dpa, the palisade cells in both cultivars always held abundant peroxidases. The intensity of peroxidase staining in the HGC of Harosoy63 was much stronger than that in palisade cells. Although the HGCs in Harosoy63 have considerable peroxidase activity, peroxidase staining was concentrated in the central vacuole (Fig. 3.9(1)). The HGC of Jack had a much lower intensity of peroxidase staining than that in palisade cells. Most peroxidase staining was observed on the cell walls, and little peroxidase staining showed in the cytoplasm of the HGCs in Jack (Fig. 3.9(2)).

Of course, leakage can be a problem. When we section fresh tissues, it is hard to avoid breaking the cells, which could cause peroxidase leakage among different cells and

even within individual HGCs. So, these confocal results just show us probable changes of SBP in HGCs. Leakage will be further discussed later.

These results confirm those of Gijzen et al. (1993) and indicate that SBP, encoded by *Ep*, is not the only peroxidase in soybean seed coat and there are some other peroxidases in palisade layers.

Figure 3.7 Confocal micrograph of a cross section through 12dpa hourglass cells

Cross section of hourglass cells at 12 days post anthesis, stained with chloronaphthol. 1) Harosoy 63. 2) Jack. (A)The confocal / fluorescence image. (B) The bright field image. (C) The chloronaphthol fluorescence image.

P, palisade layer; H, hourglass cell.

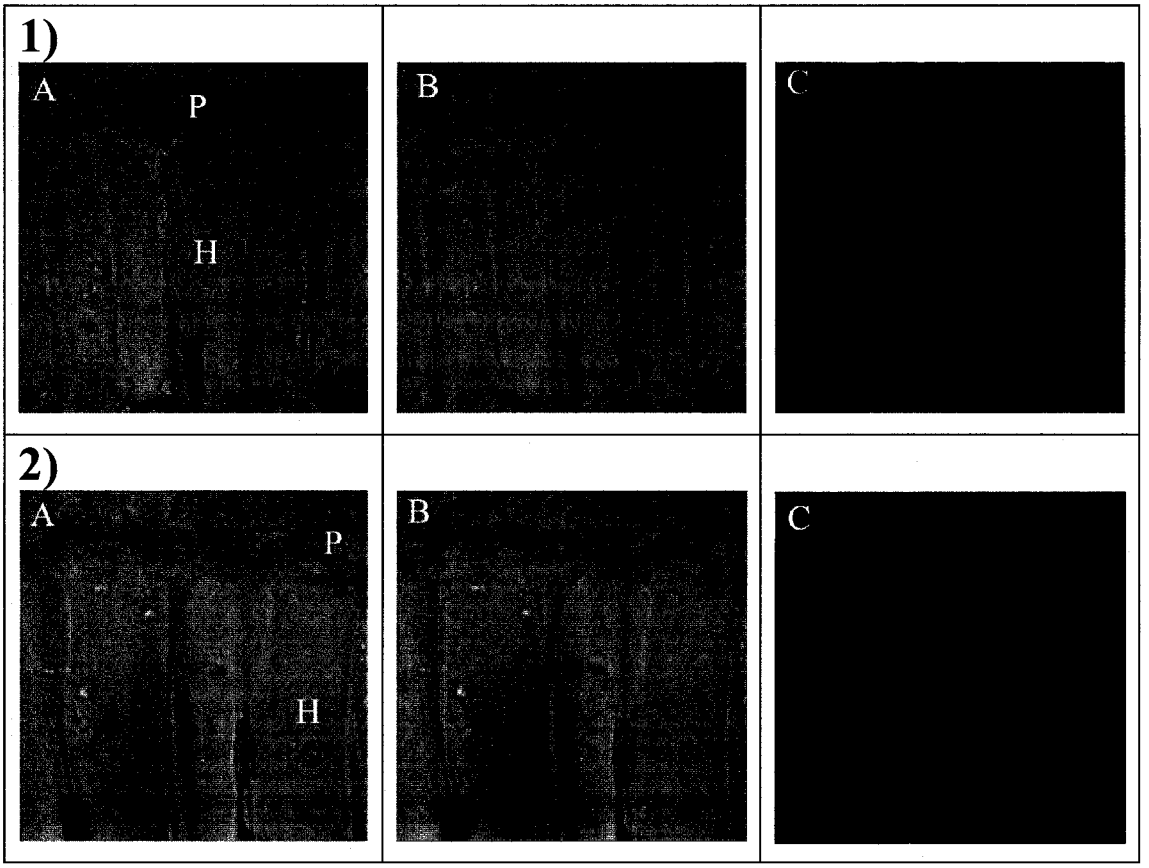
1)
A
P
H
B
C
2)
A
P
H
B
C

Figure 3.8 Confocal micrograph of a cross section through 19dpa hourglass cells

Cross section of hourglass cells in Jack at 19 days post anthesis, stained with chloronaphthol. 1) Harosoy 63. 2) Jack. (A)The confocal / fluorescence image. (B) The bright field image. (C) The chloronaphthol fluorescence image.

P, palisade layer; H, hourglass cell.

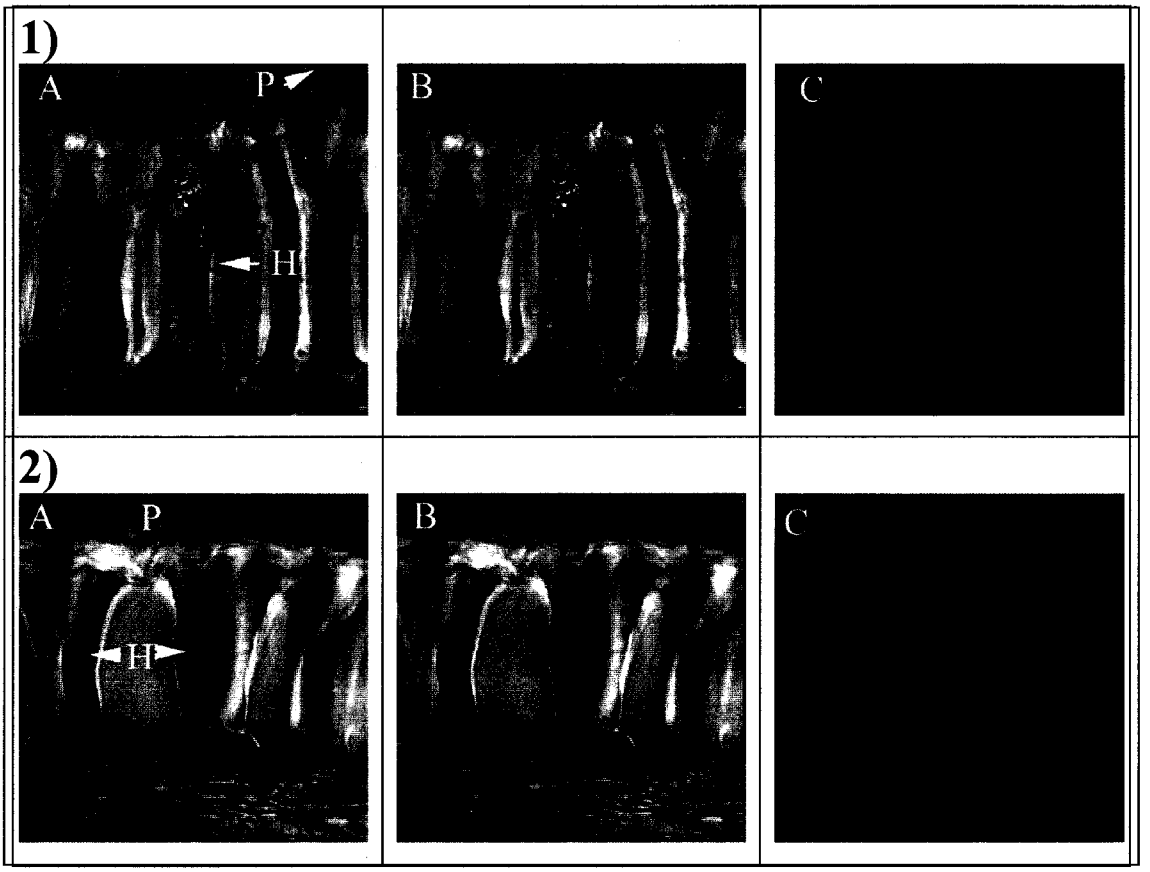
1)
A
P
H
B
C
2)
A
P
H
B
C

Figure 3.9 Confocal micrograph of a cross section through 30dpa hourglass cells

Cross section of hourglass cells at 30 days post anthesis, stained with chloronaphthol. 1) Harosoy 63. 2) Jack. (A)The confocal / fluorescence image. (B) The bright field image. (C) The chloronaphthol fluorescence image.

P, palisade layer; H, hourglass cell.

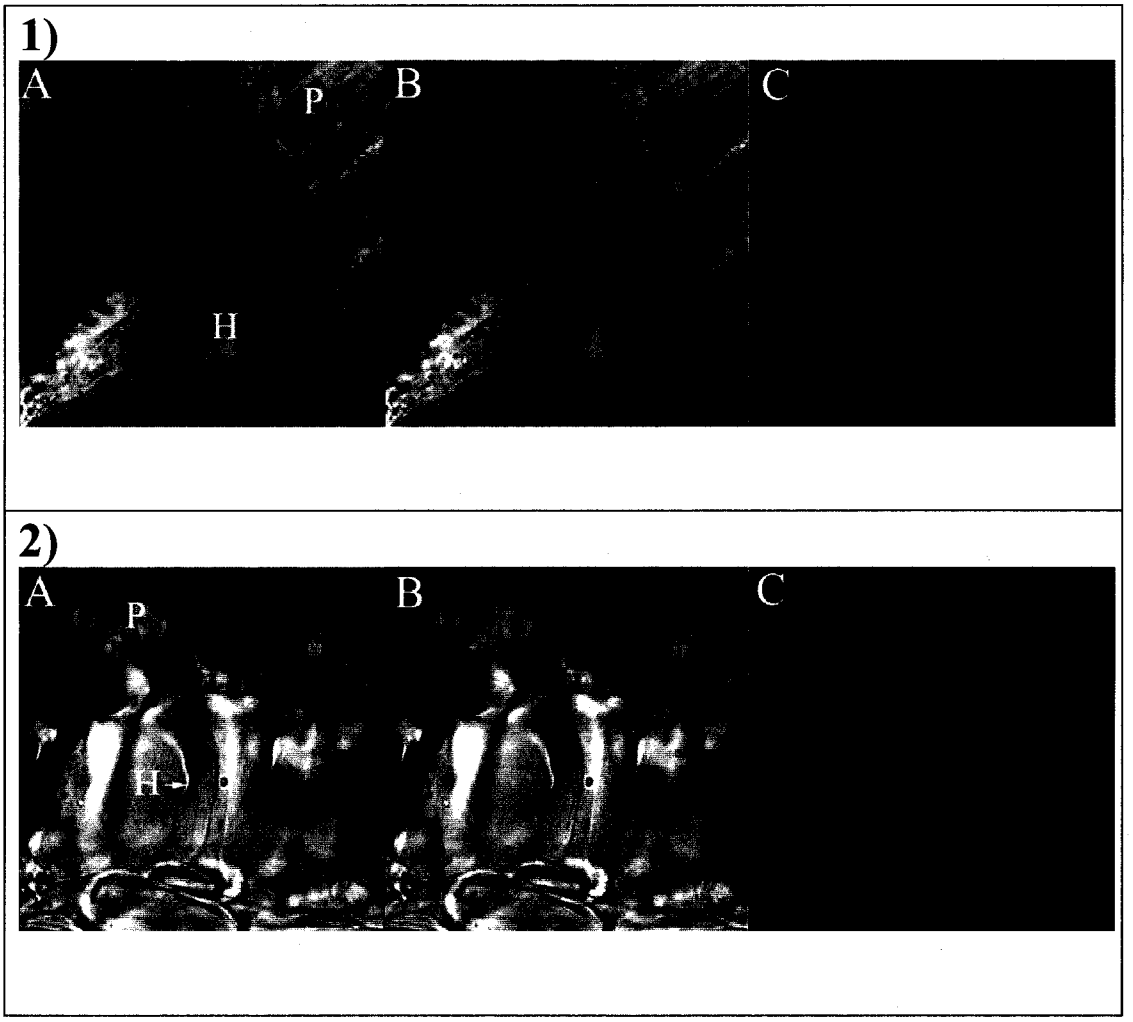
1)
A
P
B
C
H
2)
A
P
B
C
H

3.7 The Small Vesicles in Soybean Cotyledon Cells

Because no distinct protein storage vesicles were detected in the hourglass cells in any of the micrographs from brightfield, confocal or TEM, an experiment was conducted to determine whether protein storage vesicles could, in fact, survive the sample preparation protocols used. For this work, soybean cotyledon, which is known to contain storage protein bodies, was used. Fresh cotyledon sections of mature but still green soybeans were stained with Neutral Red, and examined using a Confocal microscope. For examination of fresh cotyledons, an unspecified soybean cultivar from Dr. E. Cober (Agriculture and Agri-Food Canada, Ottawa, ON, Canada) was used. Then, fixed and embedded cotyledon tissues at of Maple Presto 15 dpa and 18 dpa were observed by TEM and SEM.

By using Neutral Red and Confocal microscopy, numerous small vesicles (black arrows) were detected in the cotyledon cells of the mature soybean (Fig. 3.10(1)). By using SEM, large numbers of small protein vesicles and larger starch grains were found in the cytoplasm of the cotyledon cells in the soybean at 18 dpa, although the central vacuole was still very large in the cell (Fig. 3.10(2)). Similarly, abundant small electron semitransparent vesicles were observed in the cytoplasm of the cotyledon cells at 15 dpa (Fig. 3.10(3)). The ultrastructural evidence, combined with Neutral Red staining, suggests that these small vesicles are in fact protein storage vesicles.

Although we were able to observe protein storage vesicles in the cotyledon cells using Confocal microscopy, TEM and SEM, we only observed a few similar structures in the hourglass cells at 21 dpa using the same preparation protocols. Thus we concluded that the HGCs do not contain many protein storage vesicles during their development.

Figure 3.10 Cotyledon cells in soybean

1) Cross section of cotyledon cells in mature soybean, stained with Neutral Red. (A)The confocal / fluorescence image. (B) The bright field image. (C) The Neutral Red fluorescence image. Small vesicles (black arrows). 2) Scanning electron micrograph of hourglass cells at 18 days post anthesis. 3) Transmission electron micrograph of hourglass cells at 15 days post anthesis.

CW, cell wall; V, vacuole; C, chloroplast; ER, endoplasmic reticulum; s, starch grain; psv, protein storage vesicles.

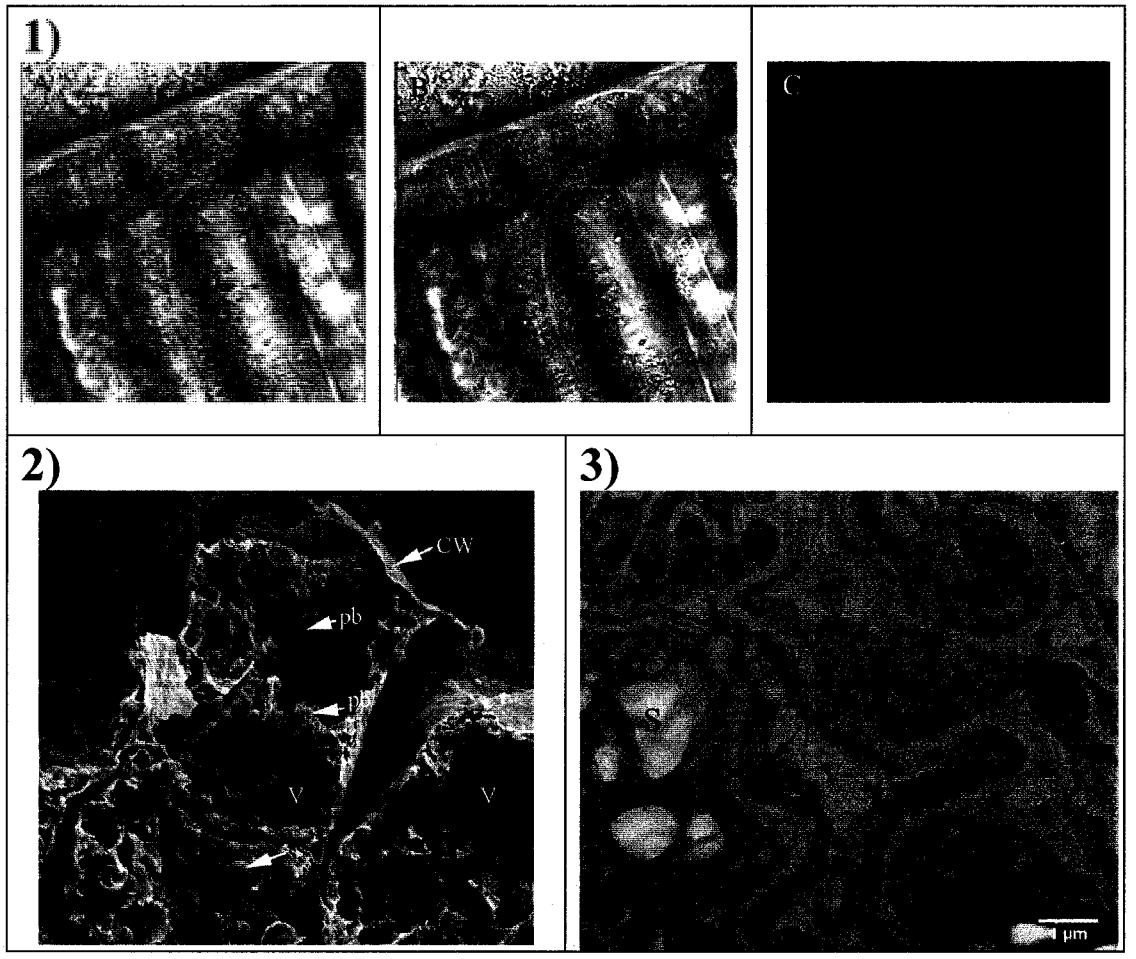
1)
A
B
C
2)
CW
pb
pb
V
V
3)
S
µm

CHAPTER FOUR: DISCUSSION

The first goal of the present study was to investigate hourglass cell development in the soybean seed coat. Their structures were studied during the early phases of seed coat development by transmission electron microscopy, scanning electron microscopy, confocal microscopy and light microscopy. The localization of SBP in HGCs was studied using confocal microscopy.

Before considering the function of HGCs in soybean seed coats, a summary of the results of this research will be presented. In this context, the problem of leakage of SBP from organelles and cells will be analyzed. The possibility that HGCs may be undergoing programmed cell death during the soybean seed coat development will be discussed. Then, the hypothesis that SBP crosses from ER to Golgi to vacuole in the endomembrane system of HGCs will be discussed. Finally, the conclusions and future work are outlined.

4.1 Summary of Results

The ultrastructure of HGCs from 9 dpa to 45 dpa was studied in this work. During soybean seed coat development, HGCs show different views at different stages. The characteristic hourglass cell shape, thick and strong cell walls, intercellular air spaces and large central vacuoles are the main morphological features of the mature HGC.

At 9 dpa, HGCs are undifferentiated plant cells. There are no clear differences with other cells in the palisade and parenchyma layers. From 12 dpa to 15 dpa, HGCs are differentiating. The lumen is primarily occupied by a large central vacuole in which many vacuolar inclusions are beginning to accumulate, cell walls are becoming thick, HGCs are assuming the hourglass shape and clear air spaces are showing between them. From 18 dpa

to 21dpa, HGCs are well defined. Their cell walls become thicker and have a layered appearance. Central vacuoles occupy most of the cell lumen. The nucleus and cytoplasm containing several mitochondria, ER, chloroplast, starch grains and Golgi are concentrated in the remaining volume. Vacuolar inclusions are found in the central vacuole. Some small electron opaque vesicles are found in the cytoplasm of both HGCs and parenchyma cells. From 24 dpa to 30 dpa, the ultrastructure of HGCs changes. Most vacuolar inclusions are degraded, and only a few remnants persist in the central vacuole. The cytoplasm and the central vacuole are fusing together. The number of organelles of all types is declining. At 45 dpa, little ultrastructure remains in the HGCs. All organelles in HGCs appear to have been degraded, and their remnants fill the whole central vacuole.

During HGC development, the overall shape and size of an HGC changes from a small, rectangularly shaped plant cell to a large hourglass-shape cell. We did not attempt to accurately document these changes since it is hard to ensure that all slices are sectioned at the same angle and that all tissues are taken from the same region of the seed coat. The sizes of HGCs are different in the different areas of the soybean seed coat, where the heights of the HGC are higher near the hilum, intermediate in the central abaxial side and shorter on the dorsal side (Meyer et al. 2007). Thus measurements will not be accurate unless we could ensure that all tissues were taken from the same region of the seed coat. The same inaccuracy would occur in the sectioned angles. An alternative approach could be to count the changes of cell wall layer numbers during HGC development. Because the thick cell wall found in mature HGCs consists of multiple cell wall layers that result from deposition of thin, single layers of cell wall, the changes in the numbers of cell wall layers on the developing HGCs that can be observed by TEM could prove to be a useful marker.

Plasmodesmata connect HGCs throughout development, from 9dpa up to 45 dpa (Section 3.5). They also connect HGCs to palisade cells and parenchyma cells, and are seen between parenchyma cells. Thus all these cells are interconnected by plasmodesmata. Plasmodesmata are not degraded when plant cells die (Lachaud and Maurousset, 1996) and at 45dpa they may be a non-functional remnant that is not degraded when HGCs are dead.

As an important class of heme enzymes which contain an iron ion in their structure and are essential to a number of critical catalytic actions (McRee et al., 1994), several different peroxidases are contained in plants. SBP is a peroxidase which is encoded by *Ep* gene and is stored stably in HGCs of soybean seed hull. Peroxidases in fresh soybean seed coats were stained by chloronaphthol and detected using confocal microscopy. From 12 dpa to 30 dpa, the palisade layer in soybean seed coats always contains peroxidases, whether they are in an *EpEp* cultivar (Harosoy63) or in an *epep* cultivar (Jack). However, the expression of peroxidases in HGCs of the two cultivars is very different. A small amount of peroxidase is detected in the HGCs of the *EpEp* cultivar at 12 dpa. Much more peroxidase is found in the cytoplasm of the HGCs by 19 dpa. At 30 dpa, the *EpEp* HGCs are full of peroxidase. In contrast, no peroxidase activity is detectable in the HGCs of the *epep* cultivar at 12 and 19 dpa. At 30 dpa, some peroxidase activity is detectable on the cell wall and cytoplasm in the *epep* HGCs, which could be caused by leakage from the palisade layer. These results are consistent with the hypothesis SBP is localized to the HGC but that there are other peroxidases localized to the palisade cells of *EpEp* and *epep* soybean cultivars.

Finally, to identify if HGCs were used for nutrition storage in soybean seed coat, HGC structures were compared with cotyledon structures. A large number of protein bodies and protein storage vesicles were detected in soybean cotyledon sections, but, using the same preparation methods, only a few protein bodies and protein vesicles were found in 21 dpa

HGCs (Section 3.7). Our tentative conclusion is that the HGCs do not contain many protein storage vesicles and are not used for nutrition storage in soybean seed coat.

4.2 The Function of HGCs

The protection of the embryo and the supply of nutrients during seed development are two major functions of seed coats (Kigel and Galili, 1995). As one of the main layers in mature soybean seed coat, HGCs show special structural features, such as thick and strong cell walls, various sizes of intercellular air spaces (Meyer et al. 2007) and large central vacuoles. In our studies, the cell wall was observed to thicken during development such that it appears to consist of multiple layers (Fig 3.3 E). At later times the cell wall was too strong to be broken during SEM preparation. Thus it appears that the thick cell walls could provide HGCs with mechanical strength.

As a starch-storing organ, the legume embryo receives sucrose as the major form of photoassimilate from pods and leaves. There is significant photosynthesis by seed coats since ca 20% of the photosynthetically active radiation reaching the pod is transmitted through to the seed coat (Smith and Denyer, 1992). Nutrients arriving from leaves via the phloem have to be unloaded through the developing seed coat into the endospermal cavity before reaching the embryo. Seed coats can influence embryo development. For example, it could adjust nutrient supply as shown for carbohydrates and nitrogen. Seed coat-associated invertase is involved in controlling seed size by changing the carbohydrate state of developing seeds and triggering developmental processes (Weber et al., 1996). Frey et al. (2004) found maternal abscisic acid synthesized in the seed coat could promote its growth, avoid abortion, and regulate the embryo development in *Nicotiana plumbaginifolia*.

In my results, few starch grains and small electron opaque vesicles were observed in HGCs by TEM after 18 dpa (Fig. 3.3 F,G); the main feature of the cells being a large empty central vacuole. In contrast, large numbers of starch grains were stored in the palisade layer, even at 27 dpa (Fig 3.3 I). There are two possible reasons: 1) The starch grains may be used as a nutritional reserve for the developing embryo. The seed coats of peas are transient storage organs that accumulate starch and proteins at early stage before storage activity starts in the embryo (Weber et al., 2005), and van Dongen et al. (2003) found nutrients were transported from the ground parenchyma to the cotyledons by diffusion through the apoplastic transport in pea. The transport from soybean seed coat to its embryo is still unknown, but soybean seed coats may use the same transport between their palisade layer and cotyledons, because the seed coats of peas, being a legume, have a very similar organization to those of soybeans. And the palisade layers support more nutrients for the developing embryo than HGCs do during soybean seed development. 2) HGCs may use these starch grains for synthesis of their thick cell walls during HGC development. The plant cell wall is made up of carbohydrates, and starch grains are the major carbohydrate resources in plant cells (Geiger and Servaites, 2001). Borisjuk et al. (2005) demonstrated that starch, lipid and protein contents show a near-linear increase during early and mid-stages of soybean embryo development. From their TEM results, a lot of starch grains and PSVs were observed in soybean embryo cells in all different developing stages. Although Borisjuk et al. and I used different scales to describe different developing stages of soybean, from the sizes and colours of embryo in their paper, I could estimate primarily that their early stages is before 21 dpa, and mid- stages is between 24- 36 dpa. Comparing my TEM results with Borisjuk's, it is easy to find that HGCs just accumulate some nutrition at the early-stages of embryo development. Thus, HGCs are not a kind of cell for nutrition storage in soybean seed, though

they do supply some nutrition for the embryo at early stages of development (Algan and Buyukkartal, 2000; Wang and Grusak, 2005). Clearly, the main function of hourglass cells is maintaining the mechanical strength of the seed coat.

4.3 Leakage Problems

The effects of leakage during sample preparation on the localization of peroxidases in soybean seed coat cells are the main limitation in this thesis. I used the same staining protocol as Gijzen et al. (1993) for detecting peroxidases in soybean seed coat, but I used a vibratome to cut fresh sections, so I could control the section thickness. Although steps were taken to reduce leakage among cells when I was observing fresh sections using confocal microscopy, such as sectioning fresh samples in PBS (0.01M, pH 7.2) buffer to keep osmotic balance, which could reduce leakage inside the cells, and observing the middle cells in the stained sections, it is still hard to avoid breaking the cells. For example, it clearly shows in Fig. 3.8(2) chloronaphthol staining is only at the foot of two HGCs which are clearly sliced open. Leakage of peroxidase could vary among different cells and even among organelles within individual HGCs. These confocal results show us probable changes of the expression of peroxidases in soybean seed coat.

In the TEM and immnogold labelling work (Appendix), all samples were fixed in glutaraldehyde solution before sectioning. However, leakage is also a problem for the determination of subcellular localization of SBP in the HGC. The simplest explanation for SBP in the nucleus, chromatin, and cytoplasm in HGCs at 18 dpa is leakage. I did not have antibodies specific for organelle proteins needed to demonstrate if there is leakage from them.

4.4 Programmed Cell Death in HGCs

In plants, programmed cell death (PCD) is a process aimed at the removal of redundant, misplaced or damaged cells and maintenance of multicellular organisms (Palavan-Unsal et al., 2005). PCD plays a number of important roles in plant developmental pathways, including xylogenesis, formation of woody tissues in trees and perennials, leaf abscission, self-incompatibility, and defence responses to a wide variety of environmental stresses (Eckardt, 2006). In plant PCD, cell morphological changes are obvious. For example, increased vacuolation, an increase in electron opacity of individual cells, progressive incorporation of plasmatic components into the vacuole reminiscent of autophagy, degradation of plastids starting with hydrolysis of starch, deformation of the nucleus and gradual disappearance of chromatin, loss of tonoplast integrity and subsequent autolysis of the rest of cellular debris were observed during PCD in the floral nectary of *Digitalis purpurea* (Gaffal et al., 2007). Thus, microscopy can be used to provide support for PCD in plant cells.

From the differentiation (9 dpa) to the final degradation (45 dpa) phases of the HGCs, ultrastructural evidence of autophagy and autolysis was observed, and is discussed as follows:

(a) Increased vacuolation. The central vacuole was always increasing its size following the growth of the cell wall of HGCs from 9 dpa to 45 dpa. This is one of the earliest events observed in HGCs. During the HGCs development, the vacuoles are always filled with liquid such that they exert a significant pressure against the cell wall, which helps maintain the structural integrity of the plant, along with the support from the cell wall, and enables the cell to grow much larger without having to synthesize new cytoplasm. Significant changes in the

vacuome which is a system of vacuoles, usually in the form of increased vacuolation, have been widely reported in plant PCD (Rogers, 2005; Gaffal et al., 2007).

(b) Autophagy. Autophagy is a cellular process that causes degradation of long-lived proteins (Yu et al., 2006). Vacuolar autophagy in plants is involved in developmental processes such as vacuole formation, deposition of seed storage proteins and senescence, and in the response of plants to nutrient starvation or pathogens (Bassham et al., 2006). At 9 and 12 dpa, there were no vacuolar inclusions in the central vacuole. From 15 dpa to 21 dpa, abundant vacuolar inclusions were found in the central vacuole. After 24 dpa, these vacuolar inclusions were degraded quickly. At 45 dpa, the HGCs died and only a few remnants of vacuolar inclusions remained in them. The vacuolar inclusions have undergone three processes: deposition of protein, degradation of protein, and senescence. So, degradation of vacuolar inclusions seems to occur through autophagy (Gaffal et al., 2007). This process is normally used for recycling cellular components, withdrawing nutrients and extending the survival of the dying cells (Lam, 2004). General proteolytic degradation of protein is observed in cells undergoing PCD (Swidzinski et al.2004). However, HGCs still accumulate and store SBP, even after the above events have been observed. These processes need to be investigated further.

(c) Degradation of cytoplasm. The central vacuole, as a lytic compartment of plant cells, contains hydrolytic enzymes. Cytoplasm is always fused with the central vacuole during the PCD process. Starch degradation is the first obvious symptom in HGCs. There were many starch grains in the cytoplasm of HGCs from 9 dpa to

15 dpa. But few starch grains were observed in HGCs after 18 dpa; instead the primary morphological feature was a large empty central vacuole. The starch degradation in the vacuole may result in lower cell turgor and plasmolysis, which will cause premature death (van Doorn and Woltering, 2005). Degradation of starch is considered to be a morphological feature of PCD in plant cells (Gaffal et al., 2007). Cytoplasm, containing lots of mitochondria, ER, chloroplasts and Golgi, began to mix with the central vacuole contents at 24 dpa. At 30 dpa, little cytoplasm remained in the HGCs. Ultimately, no cytoplasm could be found in HGCs at 45 dpa. Although some materials still remained in the HGCs, they looked like the vacuole contents. Degradation of cytoplasm is one of the hallmarks of PCD in HGCs.

(d) Nuclear degradation. Nuclear degradation is a relatively late event in most senescing cells. Degradation of the nuclei was observed in HGCs at 45 dpa.

These symptoms are common in plants and similar to the phenotypes of senescence in the nectary of *Glycine max* (Horner et al., 2003) and *Digitalis purpurea* (Gaffal et al., 2007). Senescence is considered to be a type of PCD (Eckardt, 2006). Although there is some morphological evidence that HGCs undergo PCD during soybean seed coat development, these results still lack biochemical and molecular proof to confirm PCD in HGCs. One of my future proposals is to solve this problem.

4.5 SBP in the Endomembrane System of HCGs

SBP, encoded by the *Ep* gene, was studied in the endomembrane system of HGCs in Harosoy63 (*EpEp* cultivar) and Jack (*epep* cultivar) by using the rabbit anti-SBP antibody

(Appendix). Although leakage is a problem in this experiment, we still can get some information from the results for discussing our hypothesis.

The plant endomembrane system is responsible for both synthesizing and storing the large amount of storage proteins produced during seed development (Shewry et al. 1995). Proteins secreted from cells are collectively termed secretory proteins (Vitale and Hinz, 2005) and are stored in different compartments of the plant endomembrane system (Washida et al., 2004). The plant ER is a major site of protein synthesis, folding, assembly, and storage, and is also the first organelle in the secretory pathway (Vitale and Raikhel 1999; Staehelin 1997). The Golgi is located between the ER and the vacuole and plays a central role in the glycosylation, sorting, and transport of soluble cargo proteins in the endomembrane pathway (Neumann et al. 2003; Hawes 2005). The vacuole, including both LV and PSV, is the terminal station for secretory proteins. SBP, encoded by the *Ep* gene, was detected in the endomembrane system of HGCs of *EpEp* cultivars during soybean seed coat development. Before 15 dpa, no SBP was detected in the endomembrane system (Fig. A1.1). At 18 dpa, amount of SBP signal was found in the ER and Golgi, and a small amount of SBP signal was in the central vacuole (Fig. A1.2). In addition, I did not find many protein storage vesicles during HGC development. From 21 dpa to 30 dpa, a lot of SBP was detected on ER, Golgi and central vacuole (Fig. A1.3-1.5). At the same stages, the ultrastructure results showed that the cytoplasm and the central vacuole were mixed together after 24 dpa. Few protein bodies and protein vacuoles were found in HGCs during soybean seed coat development, which means SBP could not be stored in PSVs in HGCs. So, these results may support two possible secretory pathways for the SBP in the endomembrane system of HGCs: 1) The Golgi dependent dense vesicle pathway. In this pathway, SBP was synthesized in the ER, moved through the Golgi and stored in the central vacuole; 2) The autophagic pathway. In this

pathway, SBP was synthesized in the ER, moved through the Golgi, and entered into the central vacuole directly via cell autophagy.

4.6 Conclusions and Future Work

The results presented in this thesis show that the ultrastructure of HGCs changes during soybean seed coat development. Although more ultrastructure features in the palisade and parenchyma layers are required to complete developmental description in soybean seed coats, the studies reported in this thesis have helped to understand the complexity of HGC structure changes during seed coat development.

There are many future directions for this work including:

- an effective way to detect the leakage in HGCs and avoid leakage as happened in SBP (the *Ep* gene encoded) localization experiments should be found. Once I can localize SBP in HGC development, knowledge of secretory pathways of SBP in the HGC endomembrane system will not only outline the protein pathway in the HGCs of soybean seed coat development, but help to increase the potential of soybean transgenic technology;

-further work to look for the presence or absence of protein storage vesicles in HGCs at different times to strengthen our conclusions derived from observation at 21 dpa;

-biochemical and molecular experiments for determining PCD in HGC development should be done. At the DNA level, these should include electrophoresis of DNA to detect DNA laddering and terminal deoxynucleotidyl transferase-mediated dUTP nick end labeling (TUNEL) to detect DNA breaks. At the protein level there is a need to resolve the question of how does SBP accumulate while PCD is occurring when PCD is normally associated with protein degradation. While SBP could simply be resistant to cleavage or during PCD in HGCs the amount of degradation could be much lower than in other systems, this issue needs

to be settled. One approach to solving this problem would be to investigate general protein degradation in HGCs during development (Lam, 2004; Swidzinski, et al., 2004) and at the same time use specific antibodies to monitor the fate of proteins known to be localized to specific organelles such as the nucleus, mitochondrion, plastid and vacuole. Stronger and more direct proof for PCD in HGCs will help us to better understand the development of HGCs.

REFERENCES:

Alesandrini F, Mathis R, Van de Sype G; Hérouart D; Puppo A (2003) Possible roles for a cysteine protease and hydrogen peroxide in soybean nodule development and senescence. New Phytologist 158 (1): 131-138

Algan G, Buyukkartal HNB (2000) Ultrastructure of seed coat development in the natural tetraploid *Trifolium pratense* L. Journal of Agronomy and Crop Science-Zeitschrift Fur Acker Und Pflanzenbau 184: 205-213

Bassham DC, Laporte M, Marty F, Moriyasu Y, Ohsumi Y, Olsen LJ, Yoshimoto K (2006) Autophagy in development and stress responses of plants. Autophagy 2: 2-11

Bethke PC, Jones RL (2000) Vacuoles and prevacuolar compartments. Current Opinion in Plant Biology 3: 469-475

Boesewinkel FD, Bouman F (1995) The seed: structure and function. — In Negbi, M., Kigel, J., (Eds): Seed development and germination, pp. 1–24. — New York, Basel, Hong Kong: Marcel Dekker.

Borisjuk L, Nguyen TH, Neuberger T, Rutten T, Tschiersch H, Claus B, Feussner I, Webb AG, Jakob P, Weber H, Wobus U, Rolletschek H (2005) Gradients of lipid storage, photosynthesis and plastid differentiation in developing soybean seeds. New Phytologist 167: 761-776

Brandizzi F, Irons SL, Johansen J, Kotzer A, Neumann U (2004) GFP is the way to glow: bioimaging of the plant endomembrane system. Journal of Microscopy-Oxford 214: 138-158

Carpita NC, Gibeaut DM (1993) Structural models of primary cell walls in flowering plants: consistency of molecular structure with the physical properties of the walls during growth. Plant Journal 3: 1-30

Chrispeels MJ, Maurel C (1994) Aquaporins - the molecular-basis of facilitated water-movement through living plant-cells. Plant Physiology 105: 9-13

Claude SJ, Marie-Agnes G, Catalina R, Nadine P, Marie-Christine KM, Jean-Marc N, Loic F, Veronique G (2005) Targeting of proConA to the plant vacuole depends on its nine amino-acid C-terminal propeptide. Plant Cell Physiology 46: 1603-1612

Clements JC, Zvyagin AV, Silva KKMBD, Wanner T, Sampson DD, Cowling WA (2004) Optical coherence tomography as a novel tool for non-destructive measurement of the hull thickness of lupin seeds. Plant Breeding 123: 266-270

Corner.EJH. (1951) The leguminous seed. Phytomorphology 1: 117-150

Cosgrove DJ (2001) Wall structure and wall loosening. A look backwards and forwards. Plant Physiology 125: 131-134

Dowd PF, Lagrimini LM (1997) The role of peroxidase in host insect defenses. In: Carozzi N, Koziel M (eds) Transgenic plants for control of insect pests. Taylor and Francis, New York, pp 195-223

Eckardt NA (2006) Programmed cell death in plants: A role for mitochondrial-associated hexokinases. Plant Cell 18: 2097-2099

Egley GH, Paul RN, Vaughn KC, Duke SO (1983) Role of peroxidase in the development of water-impermeable seed coats in *Sida Spinosa* L. Planta 157: 224-232

Ene-Obong EE, Okoye FI (1993) Effect of seed coat on water permeability in the African yam bean, *Sphenostylis stenocarpa*. Nigerian Journal of Botany 6: 43–51

Flint O (1994) Food Microscopy: a manual of practical methods using optical microscopy. ßios Scientific Publishers, Oxford, UK, pp 125.

Frey A, Godin B, Bonnet M (2004) Maternal synthesis of abscisic acid controls seed development and yield in *Nicotiana plumbaginifolia*. Planta 218: 958-964

Fry SC (1986) Cross-lnking of matrix polymers in the growing cell-walls of angiosperms. Annual Review of Plant Physiology and Plant Molecular Biology 37: 165-186

Gaffal KP, Friedrichs GJ, El-Gammal S (2007) Ultrastructural evidence for a dual function of the phloem and programmed cell death in the floral nectary of digitalis purpurea. Annals of Botany 99: 593-607

Geiger DR and Servaites JC (2001) Starch and starch grains. Encyclopedia of Life Sciences 1: 1-4

Giberson RT, Demaree RS, Jr., Nordhausen RW (1997) Four-hour processing of clinical/diagnostic specimens for electron microscopy using microwave technique. Journal of Veterinary Diagnostic Investigation 9: 61-67

Gijzen M (1997) A deletion mutation at the ep locus causes low seed coat peroxidase activity in soybean. Plant Journal 12: 991-998

Gijzen M, Miller SS, Bowman LA, Batchelor AK, Boutilier K, Miki BLA (1999) Localization of peroxidase mRNAs in soybean seeds by in situ hybridization. Plant Molecular Biology 41: 57-63

Gijzen M, Vanhuystee R, Buzzell RI (1993) Soybean seed coat peroxidase - a comparison of high-activity and low-activity genotypes. Plant Physiology 103: 1061-1066

Gillikin JW, Graham JS (1991) Purification and developmental analysis of the major anionic peroxidase from the seed coat of *Glycine max*. Plant Physiology 96: 214-220

Gray JS, Yang BY, Hull SR, Venzke DP, Montgomery R (1996) The glycans of soybean peroxidase. Glycobiology 6: 23-32

Green FJ (1990) The Sigma-Aldrich handbook of stains, dyes and indicators. Aldrich Chemical Company, Inc., Milwaukee, WI

Gupta S, Shih DS, Shih CT (1985) A comparative-study on the translation of cardiovirus RNAs in rabbit reticulocyte lysates. Virology 144: 523-528

Harris WM (1984) On the development of osteosclereids in seed coats of *Pisum sativum* L. New Phytologist 98: 135–141

Hatsugai N, Kuroyanagi M, Yamada K, Meshi T, Tsuda S, Kondo M, Nishimura M, Hara-Nishimura I (2004) A plant vacuolar protease, VPE, mediates virus-induced hypersensitive cell death. Science 305: 855-858

Hawes C (2005) Cell biology of the plant Golgi apparatus. New Phytologist 165: 29-44

He F, Huang F, Wilson KA, Tan-Wilson A (2007) Protein storage vacuole acidification as a control of storage protein mobilization in soybeans. Journal of Experimental Botany 58: 1059-1070

Heinlein M (2002) Plasmodesmata: dynamic regulation and role in macromolecular cell-to-cell signaling. Current Opinion in Plant Biology 5: 543-552

Henriksen A, Mirza O, Indiani C, Teilum K, Smulevich G, Welinder KG, Gajhede M (2001) Structure of soybean seed coat peroxidase: A plant peroxidase with unusual stability and haem-apoprotein interactions. Protein Science 10: 108-115

Herman EM, Larkins BA (1999) Protein storage bodies and vacuoles. Plant Cell 11: 601-613

Hiraga S, Sasaki K, Ito H, Ohashi Y, Matsui H (2001) A large family of class III plant peroxidases. Plant and Cell Physiology 42: 462-468

Hoh B, Hinz G, Jeong BK, Robinson DG (1995) Protein storage vacuoles form de-novo during pea cotyledon development. Journal of Cell Science 108: 299-310

Horner HT, Healy RA, Cervantes-Martinez T, Palmer RG (2003) Floral nectary fine structure and development in *Glycine max* L. (Fabaceae). International Journal of Plant Sciences 164: 675-690

James, C. 2006. Global Status of Commercialized Biotech/GM Crops: 2006. ISAAA Brief No.35. ISAAA: Ithaca, NY.

Jolliffe NA, Craddock CP, Frigerio L (2005) Pathways for protein transport to seed storage vacuoles. Biochemical Society Transactions 33: 1016-1018

Jurgonski LJ, Smart DJ, Bugbee B, Nielsen SS (1997) Controlled environments alter nutrient content of soybeans. Advances in Space Research 20: 1979-1988

Keegstra K, Talmadge KW, Bauer WD, Albershe.P (1973) Structure of plant-cell walls .3. model of walls of suspension-cultured sycamore cells based on interconnections of macromolecular components. Plant Physiology 51: 188-196

Kim I, Hempel FD, Sha K, Pfluger J, Zambryski PC (2002) Identification of a developmental transition in plasmodesmatal function during embryogenesis in *Arabidopsis thaliana*. Development 129: 1261-1272

Kim YH, An ES, Song BK, Kim DS, Chelikani R (2003) Polymerization of cardanol using soybean peroxidase and its potential application as anti-biofilm coating material. Biotechnology Letters 25: 1521-1524

Lachaud S, Maurousset L (1996) Occurrence of plasmodesmata between differentiating vessels and other xylem cells in *Sorbus torminalis* L. Crantz and their fate during xylem maturation. Protoplasma 191: 220-226

Lagrimini LM (1991) Wound-induced deposition of polyphenols in transgenic plants overexpressing peroxidase. Plant Physiology 96: 577-583

Lam E (2004) Controlled cell death, plant survival and development. Nature Reviews Molecular Cell Biology 5: 305-315

Levine A, Tenhaken R, Dixon R, Lamb C (1994) H_2O_2 from the oxidative burst orchestrates the plant hypersensitive disease resistance response. Cell 79 (4):583-593

Liu J, Liu H, Zhang Y, Qiu L, Su F, Li F, Su Z, Li J (2007) A simple preparation method of crystals of soybean hull peroxidase. Applied Microbiology and Biotechnology 74: 249-255

Mader M, Ambergfisher V (1982) Role of peroxidase in lignification of tobacco cells .1. oxidation of nicotinamide adenine-dinucleotide and formation of hydrogen-peroxide by cell-wall peroxidases. Plant Physiology 70: 1128-1131

Malencic D, Popovic M, Miladinovic J (2007) Phenolic content and antioxidant properties of soybean (*Glycine max* (L.) Merr.) seeds. Molecules 12: 576-581

Marty F (1999) Plant vacuoles. Plant Cell 11: 587-599

Maruyama N, Mun LC, Tatsuhara M, Sawada M, Ishimoto M, Utsumi S (2006) Multiple vacuolar sorting determinants exist in soybean 11S globulin. Plant Cell 18: 1253-1273

Matsuoka K, Bassham DC, Raikhel NV, Nakamura K (1995) Different sensitivity to wortmannin of two vacuolar sorting signals indicates the presence of distinct sorting machineries in tobacco cells. The Journal of Cell Biology 130: 1307-1318

McRee DE, Jensen GM, Fitzgerald MM, Siegel HA, Goodin DB (1994) Construction of a bisaquo heme enzyme and binding by exogenous ligands. Proceedings of the National Academy of Sciences 91: 12847-12851

Meyer CJ, Steudle E, Peterson CA (2007) Patterns and kinetics of water uptake by soybean seeds. Journal of Experimental Botany 58: 717-732

Miklas PN, Townsend CE, Ladd SL (1987) Seed coat anatomy and the scarification of *Cicer Milkvetch* Seed. Crop Science 27: 766-772

Miller SS, Bowman LAA, Gijzen M, Miki BLA (1999) Early development of the seed coat of soybean (*Glycine max*). Annals of Botany 84: 297-304

Moise JA, Han S, Gudynaite-Savitch L, Johnson DA, Miki BLA (2005) Seed coats: Structure, development, composition, and biotechnology. In Vitro Cellular & Developmental Biology-Plant 41: 620-644

Mori T, Maruyama N, Nishizawa K, Higasa T, Yagasaki K, Ishimoto M, Utsumi S (2004) The composition of newly synthesized proteins in the endoplasmic reticulum determines the transport pathways of soybean seed storage proteins. Plant Journal 40: 238-249

Neumann U, Brandizzi F, Hawes C (2003) Protein transport in plant cells: in and out of the Golgi. Annals of Botany (Lond) 92: 167-180

Nissum M, Schiodt CB, Welinder KG (2001) Reactions of soybean peroxidase and hydrogen peroxide pH 2.4-12.0, and veratryl alcohol at pH 2.4. Biochimica Et Biophysica Acta-Protein Structure and Molecular Enzymology 1545: 339-348

Palavan-Unsal, Buyuktuncer NE-D, Tufekci MA (2005) Programmed cell death in plants. Journal of Cell and Molecular Biology 4: 9-23

Paria N, Deb DK, Chattopadhyay SP (1997) Seed-coat anatomy of some Indian leguminous taxa. Journal of Plant Anatomy and Morphology 7: 46–55

Paris N, Stanley CM, Jones RL, Rogers JC (1996) Plant cells contain two functionally distinct vacuolar compartments. Cell 85: 563-572

Park M, Kim SJ, Vitale A, Hwang I (2004) Identification of the protein storage vacuole and protein targeting to the vacuole in leaf cells of three plant species. Plant Physiology 134: 625-639

Peterson CM, Mosjidis CO, Dute RR, Westgate ME (1992) A flower and pod staging system for soybean. Annals of Botany 69: 59-67

Raper CD, Jr., Patterson RP (1986) Temperature and photoperiod responses of soybean embryos cultured in vitro. Canada Journal of Botany 64: 2411-2413

Reinprecht Y, Poysa VW, Yu K, Rajcan I, Ablett GR, Pauls KP (2006) Seed and agronomic QTL in low linolenic acid, lipoxygenase-free soybean (*Glycine max (L.)* Merrill) germplasm. Genome 49: 1510-1527

Rodriguez-Pontes M (2007) Development of megagametophyte, embryo, and seed in *Senna corymbosa (Lam.)* HS Irwin & Barneby (*Leguminosae-Caesalpinioideae*). Botanical Journal of the Linnean Society 153: 169-179

Rogers HJ (2005) Cell death and organ development in plants. Current Topics in Developmental Biology 71: 225-261

Ruzin SE (1999) Plant microtechnique and microscopy. Oxford University Press, Berkeley

Serratovalenti G, Devries M, Cornara L (1995) The hilar region in *Leucaena-Leucocephala Lam* (De Wit) seed - structure, histochemistry and the role of the lens in germination. Annals of Botany 75: 569-574

Shao S, Meyer CJ, Ma F, Peterson CA, Bernards MA (2007) The outermost cuticle of soybean seeds: chemical composition and function during imbibition. Journal of Experimental Botany 58: 1071-1082

Shewry PR, Napier JA, Tatham AS (1995) Seed storage proteins - structures and biosynthesis. Plant Cell 7: 945-956

Smith AM, Denyer K (1992) Starch synthesis in developing pea embryos. New Phytologist 122: 21-33

Sornsathapornkul P, Owens JN (1999) Zygotic embryo development in a tropical Acacia hybrid (Acacia mangium Willd x A-auriculiformis A.Cunn. ex Benth.). International Journal of Plant Sciences 160: 445-458

Souza FHDd, Marcos-Filho J (2001) The seed coat as a modulator of seed– environment relationships in *Fabaceae.* Revista Brasileira de Botânica 24: 365–375

Stabell E, Upadhyaya MK, Ellis BE (1996) Development of seed coat-imposed dormancy during seed maturation in Cynoglossum officinale. Physiologia Plantarum 97: 28-34

Staehelin LA (1997) The plant ER: a dynamic organelle composed of a large number of discrete functional domains. Plant Journal 11: 1151-1165

Surpin M, Raikhel N (2004) Traffic jams affect plant development and signal transduction. Nature Reviews Molecular Cell Biology 5: 100-109

Swidzinski JA, Leaver CJ, Sweetlove LJ. (2004) A proteomic analysis of plant programmed cell death. Phytochemistry 65 (12)1829-1838

Thorne JH (1981) Morphology and ultrastructure of maternal seed tissues of soybean in relation to the import of photosynthate. Plant Physiology 67: 1016-1025

Tilney LG, Cooke TJ, Connelly PS, Tilney MS (1991) The structure of plasmodesmata as revealed by plasmolysis, detergent extraction, and protease digestion. The Journal of Cell Biology 12: 739-747

Van Dongen JT, Ammerlaan AMH, Wouterlood M, Van Aelst AC, Borstlap AC (2003) Structure of the developing pea seed coat and the post-phloem transport pathway of nutrients. Annals of Botany 91: 729-737

van Doorn WG, Woltering EJ (2005) Many ways to exit? Cell death categories in plants. Trends in Plant Science 10: 117-122

Vitale A, Hinz G (2005) Sorting of proteins to storage vacuoles: how many mechanisms? Trends in Plant Science 10: 316-323

Vitale A, Raikhel NV (1999) What do proteins need to reach different vacuoles? Trends in Plant Science 4: 149-155

Wang HL, Grusak MA (2005) Structure and development of *Medicago truncatula* pod wall and seed coat. Annals of Botany 95: 737-747

Washida H, Sugino A, Messing J, Esen A, Okita TW (2004) Asymmetric localization of seed storage protein RNAs to distinct subdomains of the endoplasmic reticulum in developing maize endosperm cells. Plant Cell Physiology 45: 1830-1837

Weber H, Borisjuk L, Wobus U (1996) Controlling seed development and seed size in Vicia faba: a role for seed coat-associated invertases and carbohydrate state. The Plant Journal 10(5): 823-834

Weber H, Borisjuk L, Wobus U (2005) Molecular physiology of legume seed development. Annual Review of Plant Biology 56: 253-279

Welinder KG, Larsen YB (2004) Covalent structure of soybean seed coat peroxidase.

Wright H, Nicell JA (1999) Characterization of soybean peroxidase for the treatment of aqueous phenols. Bioresource Technology 70: 69-79

Biochimica et Biophysica Acta (BBA)-Proteins & Proteomics 1698: 121-126

Williams (1950) Structure and genetic characteristics of the soybean, Vol I. Interscience Publishers, New York

Yaklich RW, Vigil EL, Wergin WP (1998) Developmental changes of antipit cell ultrastructure in the soybean seed coat during seed maturation. Scanning Microscopy 12: 523-532

Yeung E (1990) Adhesion of endosperm cells to the inner surface of the bean seed coat. Journal of Structural Biology 105: 103-110

Yu L, Wan FY, Dutta S, Welsh S, Liu ZH, Freundt E, Baehrecke EH, Lenardo M (2006) Autophagic programmed cell death by selective catalase degradation. Proceedings of the National Academy of Sciences of the United States of America 103: 4952-4957

Zeng CL, Wang JB, Liu AH, Wu XM (2004) Seed coat microsculpturing changes during seed development in diploid and amphidiploid Brassica species. Annals of Botany 93: 555-566

Appendix-I Subcellular Localization of Soybean Peroxidase in Hourglass Cells

Previous work by several groups (Gijzen et al., 1993, 1997; Welinder and Larsen, 2004; Gray et al., 1996) had suggested that SBP would be localized to a vacuole (Introduction, 1.4). In this Appendix we describe preliminary work to test this hypothesis using immunogold labeling combined with transmission EM. An antibody against SBP (a polyclonal antiserum prepared in rabbits using protein expressed in *E. coli* and purified by M. C. Romero) was used to localize SBP within the endomembrane system of HGCs. In this thesis, both Jack (*epep* cultivar negative for SBP expression) and Harosoy63 (*EpEp* cultivar with high SBP expression) were compared at 15, 18, 21, 24 and 30 dpa. These times were chosen because Gillikin and Graham (1991) had found that SBP begins to accumulate at 21 dpa. In addition work by Jaimie Moïse in our laboratory (unpublished) has shown that in Harosoy63 SBP is detectable at 18 dpa by enzyme activity or Western blot using this antiserum.

At 15 dpa, few gold grains were detected in either Harosoy63 or Jack (Fig. A1.1). The ER, Golgi, nuclei and central vacuoles in HGCs of both varieties were compared. There was a small amount of labelling in the nuclei and vacuoles in both varieties, but most areas of the nuclei and vacuoles were clear (Fig. A1.1A, B). A small amount of SBP was detected near the ER and Golgi in HGCs of Harosoy63 but not in Jack (Fig. A1.1C, D). Thus, it appears that peroxidase status in the endomembrane systems of both Harosoy63 and Jack is similar at this stage.

At 18 dpa, many gold grains were detected in Harosoy63, but Jack was still clear (Fig A1.2). SBP was detected in the nucleus, ER and Golgi in HGCs of Harosoy63 (Fig. A1.2A, C) but most SBP was observed in the cytoplasm, with a little in the central vacuole. In contrast, the Jack samples were almost the same as the 15 dpa ones (Fig. A1.2 B, D). The results of controls (secondary antibody alone) showed there were no

significant differences between Harosoy63 and Jack (Fig. A1.2 E, F). Nor was SBP detected in palisade cells in Harosoy63 (Fig. A 1.6). Thus, I could confirm the primary antibody was specific to SBP encoded by the *Ep* gene.

At 21 dpa, more gold grains were detected Harosoy63 and Jack was still clear (Fig. A1.3). A large amount of SBP was detected on the nucleus, cytoplasm, ER, Golgi and vacuole in Harosoy63 (Fig. A1.3 A,C) while Jack was quite clean (Fig. A1.3 B, D). At 24 dpa, gold grains were detected throughout Harosoy63, while few gold grains were observed in Jack (Fig. A1.4). The distribution of grains was similar to 21dpa samples. A small amount of SBP was detected on the cytoplasm and central vacuole of Jack (Fig. A1.4 B, D).

At 30 dpa, Harosoy63 and Jack showed different results for the expression of SBP. In the endomembrane system of HGCs in Harosoy63, the nucleus contained less SBP than before (Fig. A1.5 A), and the central vacuole, including some degraded cytoplasm and vacuolar inclusions, was full of SBP (Fig. A1.5 C). In contrast, there was little SBP in the nucleus and central vacuole, which included abundant vacuolar inclusions, in the endomembrane system of HGCs in Jack (Fig. A1.5 B, D).

Figure A.1 Immunogold labelling in sections of hourglass cells in soybean seed coats.

Immunogold staining of HGC cells prepared and labeled with antibody against SPB as described in Materials and Methods, section 2.6. These examples represent 2 independent experiments with a minimum of 2 micrographs analyzed for each time point.

A.1.1 15 dpa;

A1.2 18dpa;

A.1.3 21 dpa;

A1.4 24 dpa;

A1.5 30 dpa;

A 1.6 Palisade cell in Harosoy63 at 18 dpa.

(A, C) or (A,C,E) Harosoy63. (B, D) or (B,D,F)Jack.

C, chloroplast; ch, chromatin; CW, cell wall; ER, endoplasmic reticulum; g, gold grain; G, Golgi apparatus; H, hourglass cell; i, vacuolar inclusion; N, nucleus; NL, nucleolus; NM, nuclear membrane; P, palisade layer; V, vacuole.

A1.1

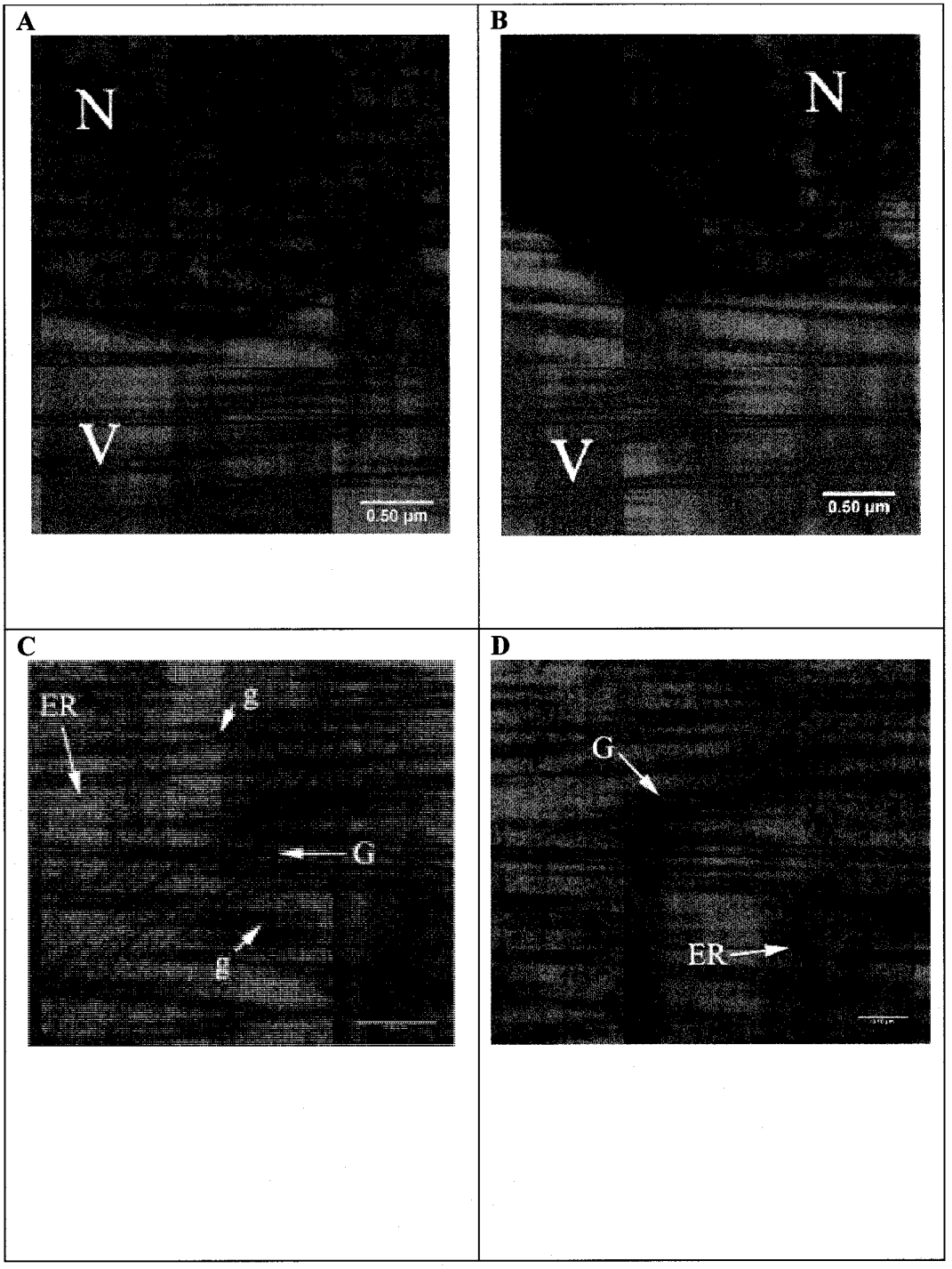

A1.2

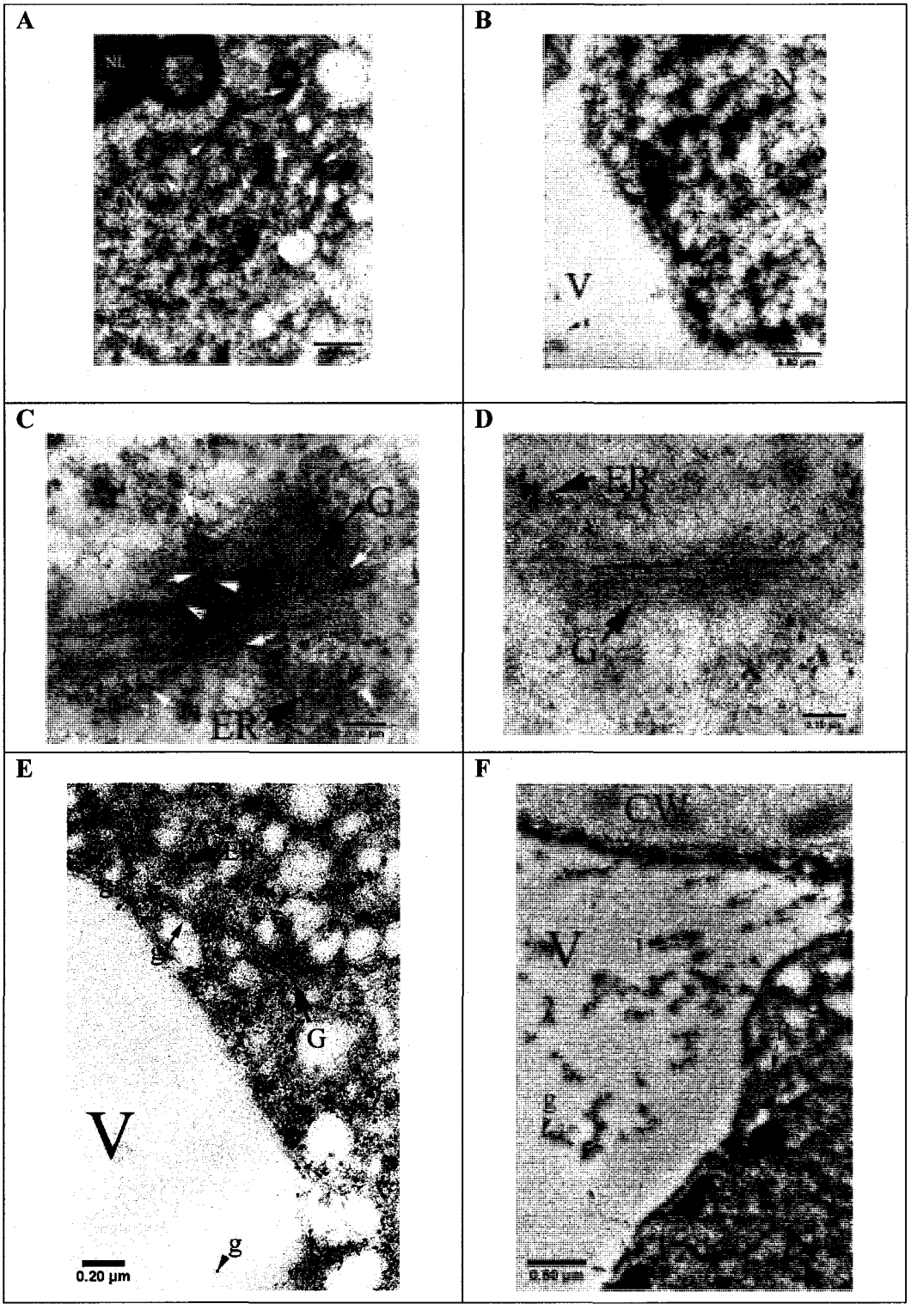

A1.3

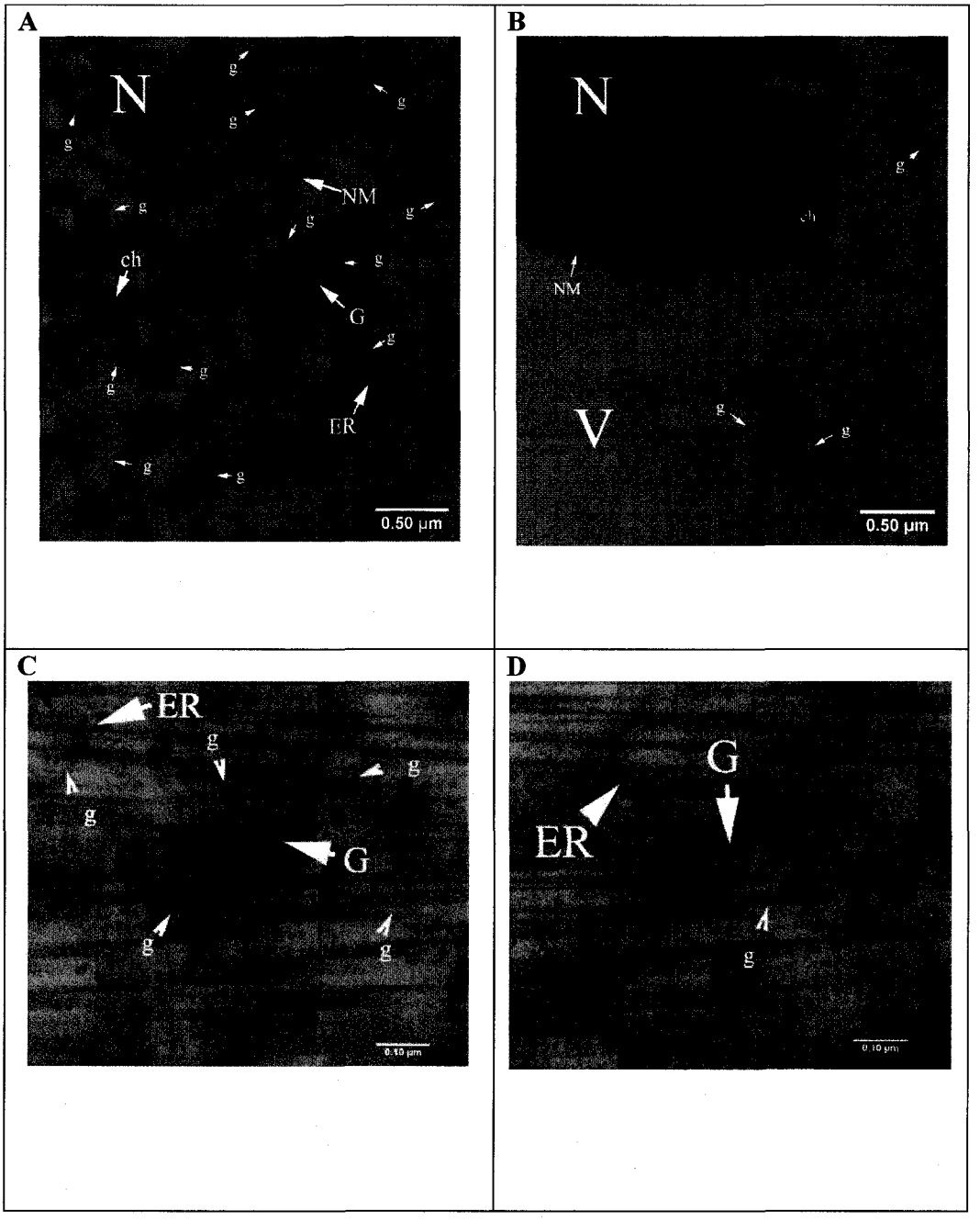

A1.4

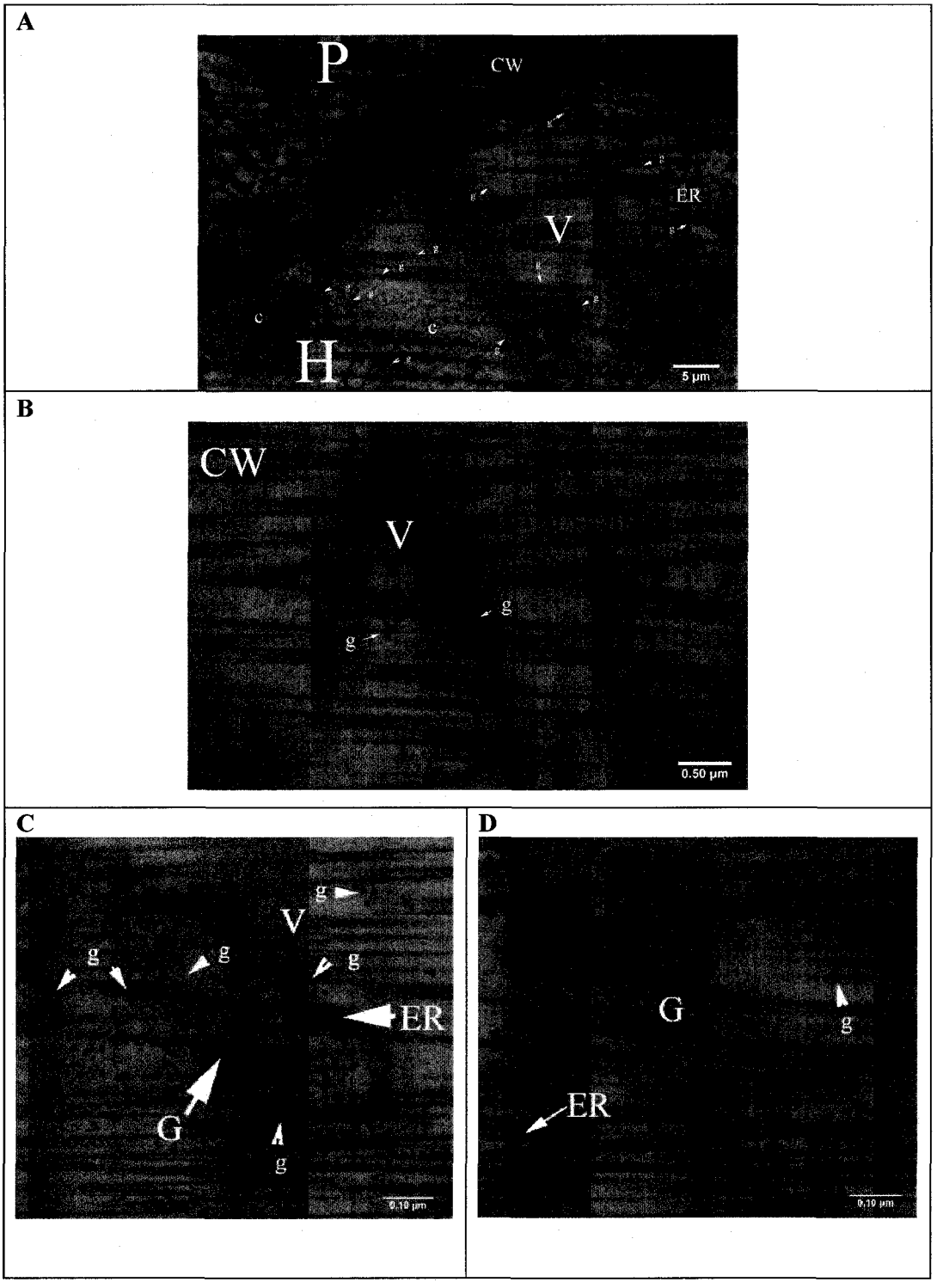

A1.5

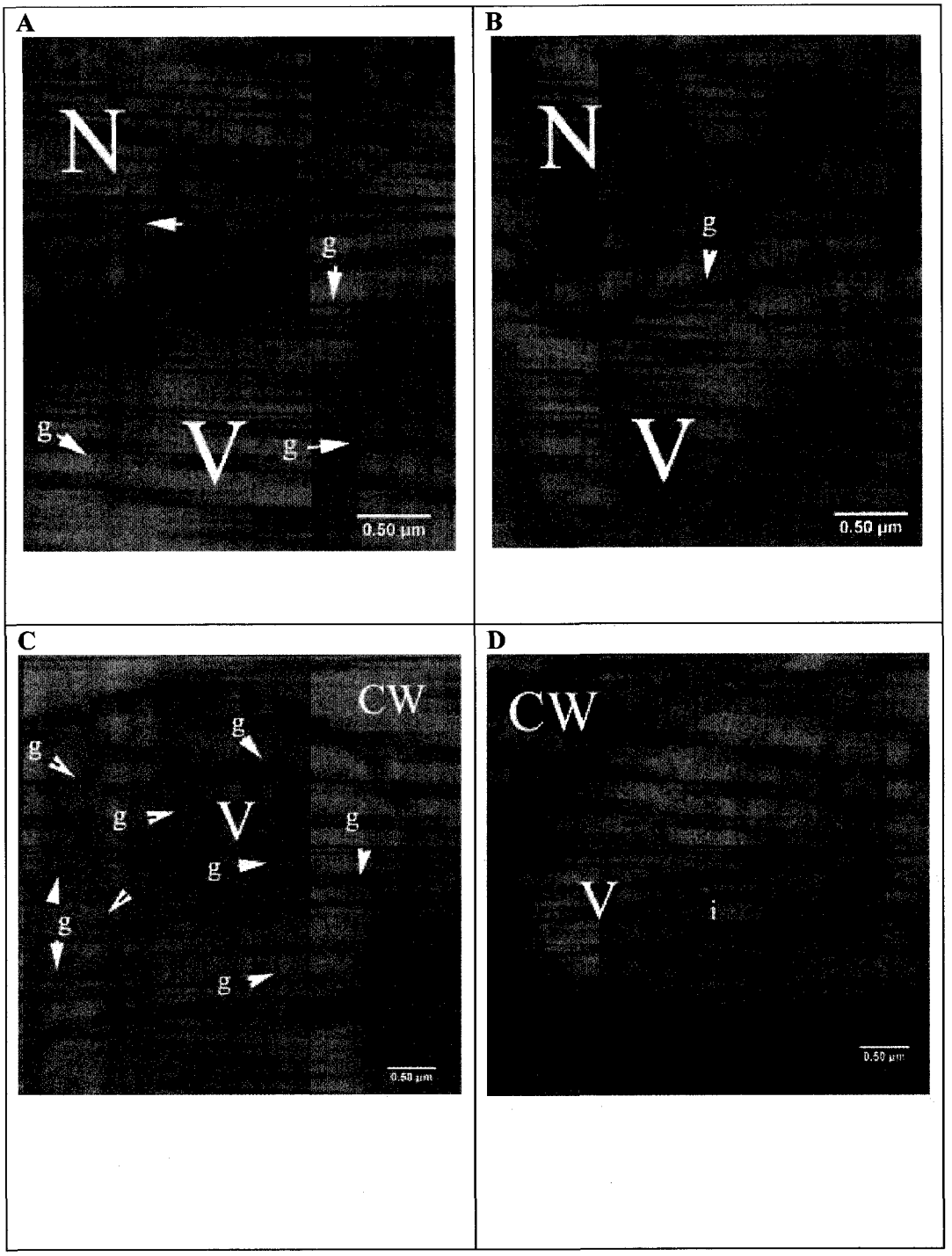

A 1.6

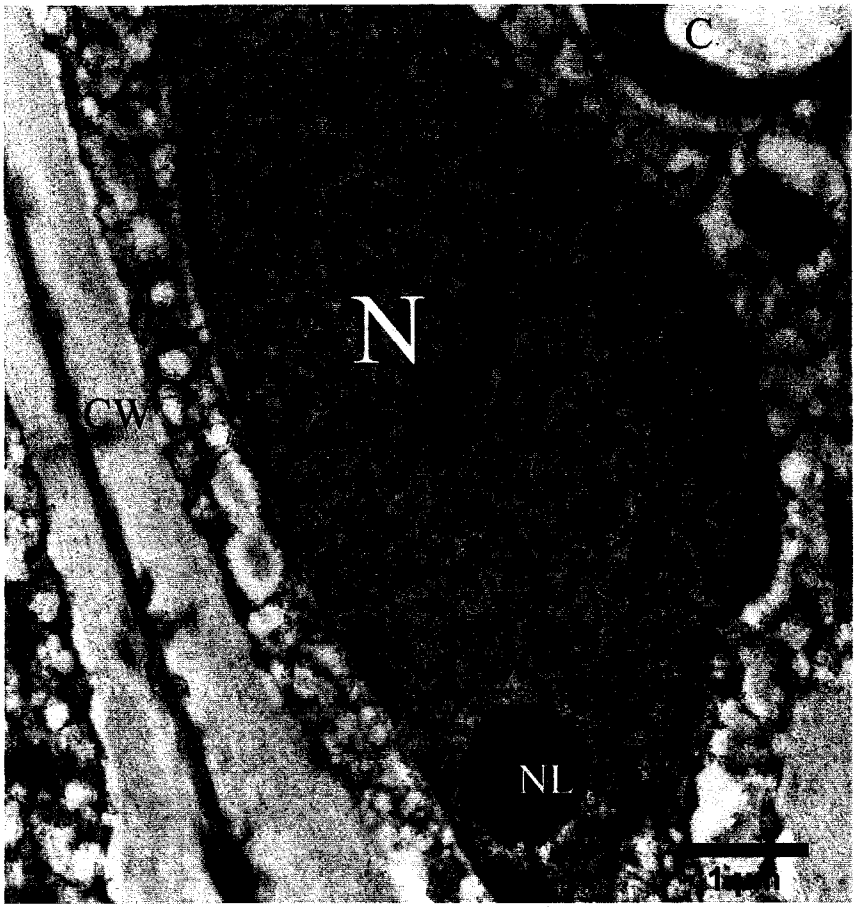

SBP, encoded by the *Ep* gene, was detected in the endomembrane system of HGCs of *EpEp* cultivars during soybean seed coat development. At 15 dpa, little SBP was detected in the endomembrane system in agreement with the protein data. At 18 dpa, SBP signals were observed on the ER and Golgi, and to a lesser extent in the central vacuole and nucleus. From 21 dpa to 30 dpa, more SBP was detected in these organelles. These results demonstrate that immunogold labeling can be used to detect SBP in the hourglass cell but that technical problems make it difficult to interpret the results. SBP was found at many locations suggesting that leakage during sample preparation may be a problem.

To complete this work more replicates must be done and more controls, including secondary antibody alone at all stages and whether SBP can be detected in parenchyma and palisade cells in Harosoy63. An effective way to rule out leakage in HGCs must be developed, e.g., antibodies specific for organelles could be used to monitor leakage.